RADIO-ASTRONOMY

SEARCH FOR THE THIRD HARMONIC OF TYPE III BURSTS RADIO EMISSION AT DECAMETER WAVELENGTHS

Brazhenko A.I. [1], Melnik V.N. [2], Konovalenko A.A. [2], Pylaev O.S. [2], Frantsuzenko A.V. [1], Dorovskyy V.V. [2], Vashchishin R.V. [1], Rucker H.O. [3]

[1] Poltava gravimetrical observatory of Institute of geophysics, National Academy of Sciences of Ukraine, Poltava, Ukraine
[2] Institute of Radio Astronomy, National Academy of Sciences of Ukraine, Kharkov, Ukraine
[3] Space Research Institute, Austrian Academy of Sciences, Graz, Austria

ABSTRACT. The results of observations of trio bursts consisting of type III bursts are presented in this paper. The instantaneous frequency ratio of trio components is near 1:2:3. We analyze flow, duration, frequency drift rate and polarization of trio components as well as dependencies of these characteristics on frequency.

Key words: type III bursts, drift rate, duration, polarization, second harmonic, third harmonic, decameter wavelength range…

The third harmonic is not usually observed in the solar type III (and associated with them) radio bursts. So new papers, reporting about registration of the third harmonic bursts, are very important for progress in theoretical aspects of researching solar corona. Detection of the third harmonic of type III bursts radio emission at decameter wavelengths can be useful for giving more precise definition to the plasma mechanism of emission and for accuracy of solar plasma parameters on relevant altitudes.

There are some records of the third harmonic in literature. Here we note a powerful U-burst recorded by Haddock and Takakura: their dynamic spectrum, presented in the monograph by Kundu (1965), shows a weak fundamental and intensive second and third harmonics. Another example is a type V burst observed by Benz (1973). Some features of dynamic spectrum of the burst are duplicated at 1.5 times higher frequencies. This indicates the presence of radio emission corresponding to the second and to the third harmonics. Also we point to numerous records of the J- and U-bursts made by Stewart (1962). Frequency ratio of that bursts lies in range 1.5-1.7. The radiation mechanism of the third harmonic was developed by Zheleznyakov & Zlotnik (1974). Afterwards this theory was improved by its authors and other scientists. For example there are papers by Takakura (1974) and Kliem (1992) based on the observations of J-bursts with frequency ratio 2:3 and the third harmonic of type II burst correspondingly. Also there are other observations of the third harmonic of type II bursts (Zlotnik 1998, Dorovskyy 2007). Only last paper refers to decameter wavelength range. Investigating the higher harmonics (Cairns 1988, Yoon 2003, Yi 2007, Rhee 2009), authors analyze similar radiation mechanisms.

Radiation mechanism

Type III radio bursts occur by so-called plasma emission. Their source is electron beam propagating along open magnetic field lines in upward direction. The propagation of electron beam through coronal plasma generates Langmuir waves (l) that can transform into escaping electromagnetic transverse waves (t) by number of processes. Fundamental plasma emission (first harmonic, t_I) results from scattering of Langmuir waves by thermal ions (i) near the local plasma frequency:

$$l + i \rightarrow t_I + i .$$

The second harmonic (t_{II}) of type III bursts occurs by coupling two Langmuir waves:

$$l + l \rightarrow t_{II} ,$$

or by coupling Langmuir wave with fundamental transverse wave:

$$l + t_I \rightarrow t_{II} .$$

It is evidently that the second harmonic radiates on double local plasma frequency.

So, the third harmonic radio emission is generated on the triple electron plasma frequency by interaction of three Langmuir waves:

$$l + l + l \rightarrow t_{III} ,$$

or by interaction of Langmuir wave and transverse wave of the second harmonic:

$$l + t_{II} \rightarrow t_{III} .$$

Observations

The bursts, we analyze in this paper, were registered during summer observations in 2011 and 2012 with the radio telescope URAN-2. It is one of the biggest radio telescopes of decameter wavelength range (effective square is 28000 m^2). URAN-2 can receive two linear (circular) polarizations. Spectrograph DSPz allows registering radiation with frequency resolution 4 kHz and time resolution 10 ms in a whole frequency band 8 – 32 MHz (or in a part of it).

We registered 12 trio composed of a combination of type III and type IIIb bursts. Observations were made in a frequency band 8 – 32 MHz with time and frequency resolution 100 ms and 4 kHz correspondingly. Example of trio consisting of IIIb-IIIb-III bursts is shown on Figure 1. We find such regularities in a structure of trio bursts: the first component was a type IIIb burst mostly, the second component was a type III burst as well as type IIIb burst, the third component was a type III burst in the most cases. Moreover, type III burst was the first component of trio only in a combination III-III-III, and type IIIb burst was the third component only in a combination IIIb-III-IIIb.

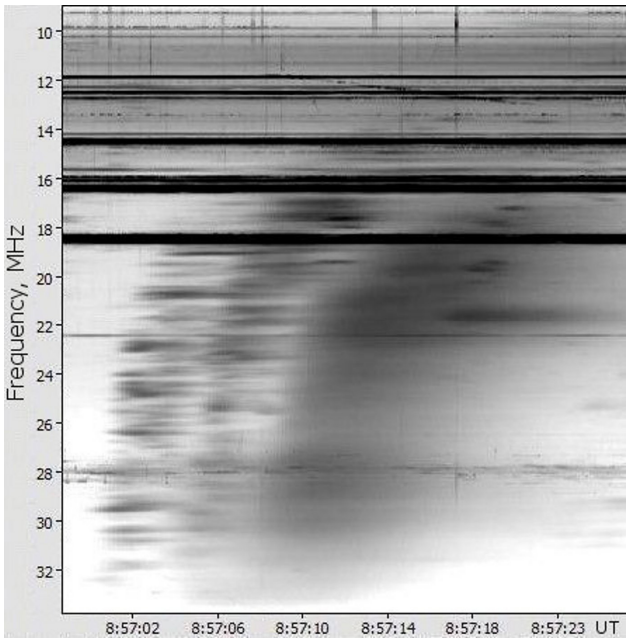

Figure 1: Example of trio.

We simulate an "average" trio for more clearly understanding the characteristic properties. The measurements of burst features, averaging in 4 MHz intervals, will be presented further.

Polarization

We find that components of each trio have the same sign of polarization. Polarization of type IIIb bursts is high, registered value is up to 60-70%. Type III bursts have smaller polarization, registered value is up to 10-20%. Polarization of the first component is always the highest in trio bursts. In addition there is a trend that the third component of trio has smaller polarization then second component (for the same type bursts).

Duration

We register duration at the level of 0.9-power, because measurements of duration were impossible at half-power level. We recalculate 0.9-power duration to half-power duration supposing that the form of burst is Gaussian. The values we derive for type III bursts vary from 2.3 s to 15 s. The most number of values concentrates in interval 5 – 10 s. The type IIIb bursts have always smaller duration at the same frequencies: from 0.5 s to 7 s. The majority of values lies in range 1.3 – 5 s.

Moreover we obtain that duration of bursts increases with decreasing of frequency. Figure 2 shows this dependency for "average" trio.

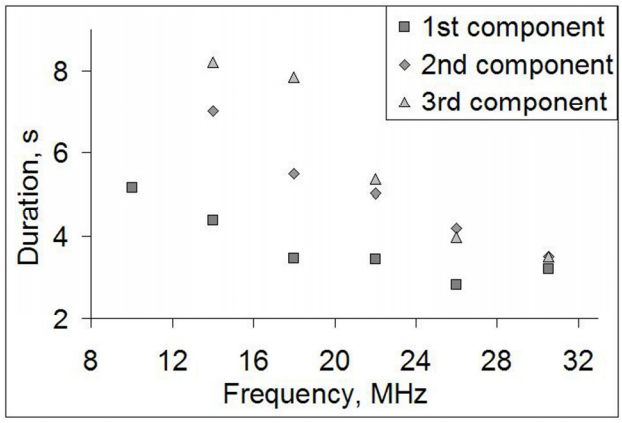

Figure 2: Average duration of trio components dependencies on frequency. Grey marks are results of measurements, that were averaging over all trio in proper frequency band

Frequency drift rate

The emission of all bursts in all registered trio drifts rapidly from high to low frequencies. The frequency drift rate decreases with decreasing frequency, its values vary from 1.1 MHz/s to 4.4 MHz/s. We find the drift rate dependence on frequency is linear:

$$df/dt = -bf \ .$$

The value of factor b lies in interval from 0.07 to 0.18. Such results are confirmed by some papers (Wild, 1950; Melnik & Boiko, 2011), whose authors independently obtain similar proportional coefficient. The factor b indicates the size of coronal inhomogeneity over the active region. The linear dependency of drift rate on frequency is evidence of exponential corona (Melnik & Boiko, 2010).

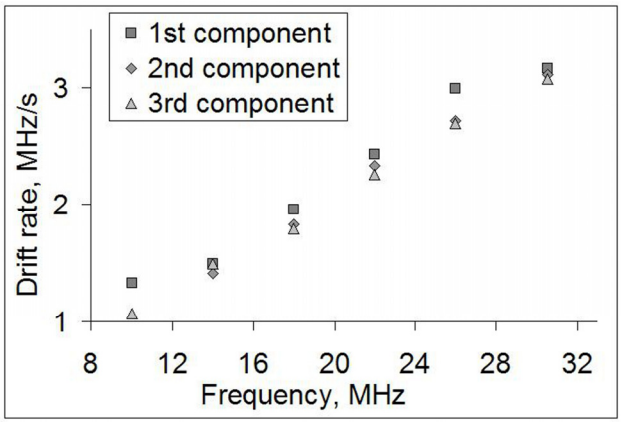

Figure 3: Average drift rate of trio components dependencies on frequency. Grey dots are results of measurements, that were averaging over all trio in proper frequency band.

Drift rate of different components of a trio differ a little in equal frequency intervals: average deviation is near 10%. Average drift rate of the first trio component is more than others. And the second trio component tends to drift faster than the third component. Figure 3 shows how drift rate of trio components depends on frequency.

Instantaneous frequency ratio

Many bursts were not visible at low frequencies through disturbances and influence of ionosphere. Therefore we have to simulate bursts to calculate the instantaneous frequency ratio.

To estimate a frequency ratio of trio components we approximate bursts (maximum flow of bursts) with different functional dependencies. The most correct model is described by the exponential function:

$$f = ae^{-bt},$$

where f – frequency, t – time of maximum flow from the beginning of the observation, a, b – coefficients calculating by the least-squares method. This conclusion is confirmed by the derived results about linear dependence of drift rate on frequency:

$$f = ae^{-bt},\ df/dt = -abe^{-bt} = -bf\ .$$

We obtain the instantaneous frequency ratio of trio components by averaging frequency ratio in points of time interval in which simulated trio arranges in frequency band 8 – 32 MHz (see Figure 4). Instantaneous frequency ratio of maximum flow of the first and the third "average" trio components is $f_3/f_1 = 2.7$. The third trio component occurs at a 1.5 times higher frequency than second component: $f_3/f_2 = 1.5$. The frequency ratio of the second and first trio components is $f_2/f_1 = 1.8$, it is confirmed by the theoretical and observational papers about the second harmonic.

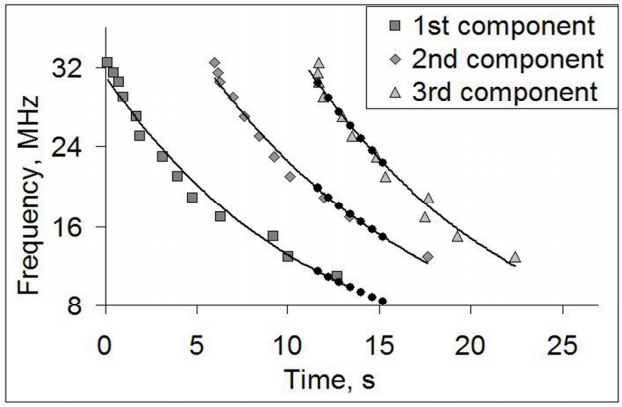

Figure 4: Approximation of trio. Grey points are average observed values of maximum flow. Curves present exponential model of bursts. The frequency ratio of trio components was calculated in black points.

So, there are a number of reasons that allow us to assert that registered trio components have harmonic relations:

1) polarization of the first component of trio is always higher than others; it is up to 60 – 70%, that corresponds to the generally accepted viewpoint about the first harmonic emission;

2) the second and the third components of trio have polarization (10 – 20%), that is typical for the second and the third harmonics according to the plasma radiation mechanism;

3) instantaneous frequency ratio is near to 1:2:3.

References

Kundu M.R.: 1965, *Solar Radio Astronomy*, Interscience Publ., New York.

Benz A. O.: 1973, *Nat. Phys. Sci.*, **242**, 39.

Stewart R.T.: 1962, *CSIRO Division of Radiophysics Report RPR*, **142**.

Zheleznyakov V.V., Zlotnik E.Ya.: 1974, *Solar Phys*., **36**, 451.

Takakura T., Yousef S.: 1974, *Sol. Phys.*, **36**, 451.

Cairns I. H.: 1988, *J. Geophys. Res.*, **93**, 858.

Kliem B., Kruger A., Treumann R. A.: 1992, *Sol. Phys.*, **140**, 149.

Yoon P.H., Gaelzer R., Umeda T., Omura Y., Matsumoto H.: 2003, *Phys. Plasmas*, **10**, 364.

Yi S., Yoon P.H., Ryu C.-M.: 2007, *Phys. Plasmas*, **14**, 013301.

Tongnyeol Rhee, Chang-Mo Ryu, Minho Woo, Helen H. Kaang, Sumin Yi, and Peter H. Yoon: 2009, *Astrophys. J.*, 694:618 625.

Zlotnik E.Ya., Klassen A., Klein K.-L., Mann G.: 1998, *A&A*, **331**, 1087.

Dorovskyy V.V., Mel'Nik V.N., Konovalenko A.A., Rucker H.O., Abranin E.P., Stanislavsky A.A., Le-cacheux A.: 2007, *European Planetary Science Con-gress*, 688.

Wild J.P.: 1950, *Aust.J.Sci.Res.*, **3**, 541.

Melnik V.N., Konovalenko A.A., Rucker H.O., Boiko A.I., Dorovskyy V.V., Abranin E.P., Lecacheux A.: 2011, *Solar Phys.*, **269**, 2.

Boiko A.I., Mel'nik,V.N., Konovalenko A.A., Rucker H.O., Abranin E.P., Dorovskyy V.V., Lecacheux A.: 2010, *PRE VII*, 367.

THE RADIO CATALOGUES OF NSS102 SURVEY AT 102.5 MHZ (LSA OF LPI, RUSSIA) FOR ALL SKY ZONE OF OBSERVATION IN $-16° \le \delta \le +82°$, AND COMPARATIVE ANALYSIS WITH OTHER RADIO CATALOGUES

R.A.Dagkesamanskii [1,3], V.A.Samodurov [1,2,4], D.R.Gadelshin [1], P.N. Semenyuk [1], E.V.Kravchenko [1]

[1] Pushchino Radio Astronomy Observatory of Lebedev Physical Institute, Russian Academy of Sciences (Pushchino, Russia)
[2] National research university Higher school of economics (Moscow, Russia)
[3] rdd@prao.ru, [4] sam@prao.ru

ABSTRACT. In this paper we report the preliminary results of the total final processing of the entire radio survey observations. They made in 1991-93by LSA of LPI that is full aperture radio telescope in the program survey of the northern sky at a frequency of 102.5 MHz. As a result, the whole sky was covered in declinations and produsedradio sources catalog in $-16° \le \delta \le +82°$.

Key words: radio survey, catalogues, radio sources

In this paper we present a beta version of the complete catalog of all the observational data - about 10 000 sources with fluxes exceeding 3 Jy for all declination zone $-16° < \delta < +82°$. Only a part of the data (for declinations +14,1°…+33,5° and +60°…+82°) published and reported previously.

The survey produced by 8-beams diagram of LSA with characteristic sizes HPBW in R.A. and declination:

$$D\_\alpha = 47' \ , \ D\_\delta = 24' \cdot \sec(Z)$$

In the paper observational methodic and processing algorithms and are described. Survey results are displayed in the form of the radio sources catalog, and the initial observation of the radio telescope scans with BSA, also as the isophotes of the observational data on the 102.5 MHz.

The preliminary version has 10187 sources with the fluxes more than 3 Jy. The numbers of radio sources with the fluxes:

$\ge$ 4 Jy - 7597 sources,
$\ge$ 5 Jy - 5738 sources,
$\ge$ 10 Jy - 2629 sources

Extended sources represented by two-dimensional oriented Gaussians. Extended sources total number is 1992 sources. The number of radio sources with the scales:

$\ge 10'$ - 1314 sources
$\ge 20'$ - 1058 sources
$\ge 30'$ - 741 source
$\ge 1°$ - 177 sources

The methods of processing of daily surveys in the mode of on-line, the first results of the identification with other radio catalogs, also as with catalogs of galaxies and quasars are discussed. According to the results of comparative analysis of cross-discussed data quality basic low-frequency catalogs: UTR (17-25 MHz), 8C (38 MHz), VLSS (74 MHz), 6C (151 MHz), Miyun survey (232 MHz) our catalogs has good flux scale as for pointed also as for extended sources.

Operating (not final) version of the catalog is available at PRAO ASC LPI:

http://astro.prao.ru/cgi/view_1.cgi?cat=nss102&mod=1

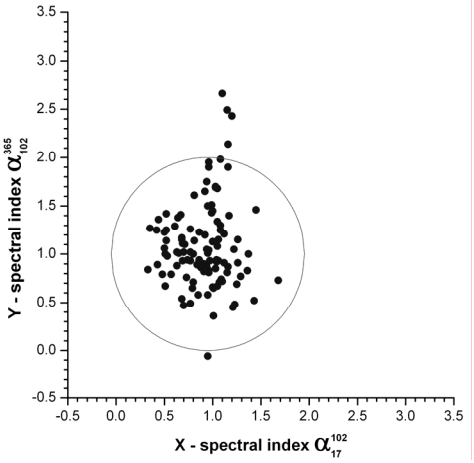

Figure 1: The example of radio sources identification in our data at 102 MHz, Txs data at 365 MHz and UTR data at 17 MHz. It represented by 2-dimentional spectral index diagram. The tail population points up are extended sources in Txs survey. NSS102 and UTR has good data agreement by small distribution spectral indexes on X.

NETWORK DEVELOPMENT OF THE PUSHCHINO RADIO ASTRONOMY OBSERVATORY OF ASC LPI

D.V. Dumsky[1], E.A. Isaev[1,2], V.D. Pugachev[1,2], V.A. Samodurov[1,2], S.F. Likhachev[3], M.V. Shatskaya[3], M.A. Kitaeva[1]

[1] Pushchino Radio Astronomy Observatory ASC LPI, Pushchino, Russia, *dumsky@prao.ru*
[2] National research university Higher school of economics, Moscow, Russia, *is@itaec.ru*
[3] Astro Space Center LPI, Moscow, Russia

ABSTRACT. All main changes in the network of the Pushchino Radio Astronomy Observatory has been related to introduction of the buffer data center in the recent years, upgrading internal and external communication channels and the exploitation of ip-telephony.

Key words: Networks: voip.

The main challenges of the buffer data center is to maintain the channels for scientific and telemetry data transfer and backup of the data in the storage as part of the space radio telescope project known as "Radioastron. The channel connects the tracking station RT-22, buffered data center, located in the territory of the observatory and data center ASC LPI, Moscow. This channel with bandwidth of 1 Gbit/s is provided by Stack Group companies and stretched using technology MPLS (Multiprotocol Label Switching) to the M9, where is connected to the ASC LPI. Currently obtained from a space telescope experimental records are passed through this channel in Moscow, and at the same time are stored in the data center buffer storage with a capacity of 20 terabytes.

However, the work buffer data center is not limited to these tasks, it is also used to host the servers that serve the local network of the observatory. Here the servers for the storage of observational data obtained from three radio astronomy systems, database servers, mail and web-server, DNS, and server of network time synchronization. Through the further development of the data center, we have increased capacity networked storage (Open-E DSS v6) from 24 to 48 terabytes, and install additional UPS for servers and switches.

A new server with two processors Intel Xeon 22.53-2.80 GHz and 12GB of RAM designed for database storage and processing of astronomical catalogs is purchased. We installed virtualization platform based on a system of native container lxc instead used on another server system Openvz to the new server. This system does not require additional manipulation with operating system kernel and further more meets the safety requirements as distributive kernel is updated more frequently than the core OpenVz. Web-servers and database server Observatory were transferred to the new system virtualization.

Additional Gigabit Ethernet managed switches to provide backup links and connect servers purchased. In order to improve ip-telephony in the Observatory, as well as voice channels with ASC LPI we replaced old Voip equipment with more reliable solution from the company addPack.

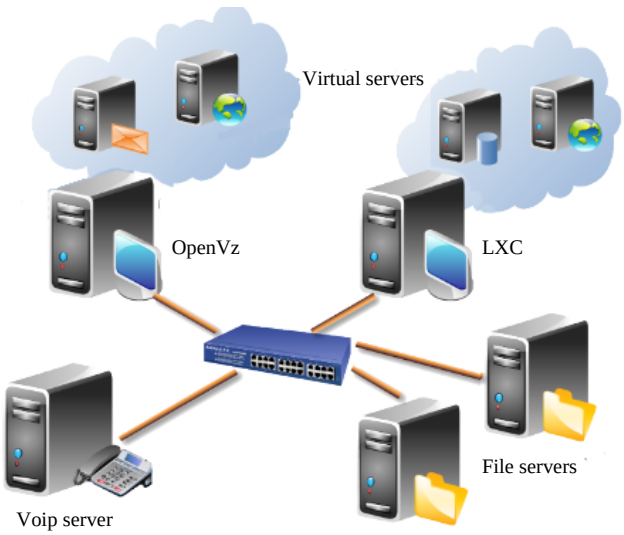

Figure 1: PRAO Data center servers

FOCUSING OF 3C144 SOURCE RADIATION BY THE SOLAR CORONA

Galanin V.V[1], Derevjagin V.G[2], Kravetz R.O[3]

Institute of Radio Astronomy of National Academy of Science of Ukraine,
Odessa, Ukraine
[1]*gvv@breezein.net,* [2]*dvg@gmail.com,* [3]*krro@ukr.net*

ABSTRACT. The research of solar corona by the compact cosmic source radiation was made on URAN-4 radio telescope. In the period from June 6 to June 20 2012 the flow of Crab nebula was measured on the 20 MHz and 25 MHz frequencies. During the eclipse we observe the great increase of 3C144 flow, which is compare with the flow of 3C461 source. Data and results of measurement analysis is presented.

Key words: radio source, solar corona.

Radio telescope URAN-4 is work in frequency range 10 to 30 MHz. Its antenna is representing the phased array with two polarizations. Its effective square is 5360 m^2 (Galanin et al., 1989). In 2010 there was perform the modernization of equipment and digital radiometer was created. In the period from June 6 to June 20 2012 on the radio telescope there was made an experiment of solar corona study by means of compact cosmic source. The observations were made in the period of solar activity maximum. We has study the transition region of solar corona with 2 to 15 solar radii, in which the solar wind is speedup.

In these days the Crab nebula 3C144 flow was measured on two frequencies 20 and 25 MHz. As a supporting source we take the CasA 3C461. Figure 1 show 3C461 to 3C144 flow ratio plots for two frequencies and two polarizations.

It's seen from this data that 3C144 flow is change from minimum, diffused, in the period from June7 to June 9, up to maximum from June 12 to June 18. In the period of maximum eclipse phase on June 15 the flow of 3C144 exceed near 4 times the flow of supporting source.

Figure 2 show records of sources 3C144, 3C274, 3C405 and 3C461 which were made from June 14 to June 15 2012.

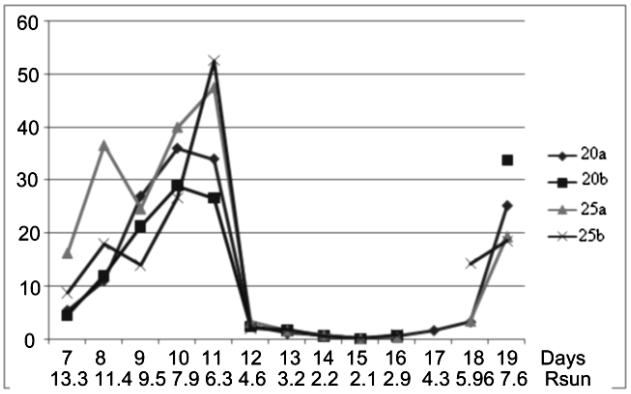

Figure 1: Ratio of 3C461 to 3C144 flow for two frequencies and two polarizations.

References

Galanin V.V. et al.: 1989, *Kinematika i fizika nebesnyh tel*, **5**, 5, 87.

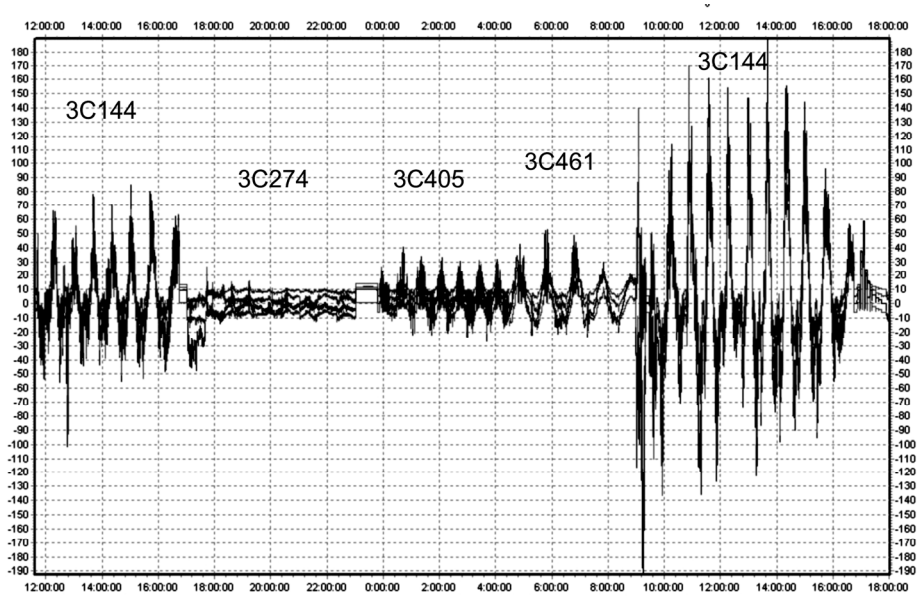

Figure 2: Records of sources 3C144, 3C274, 3C405and 3C461 from June14 to June 15 2012.

DATA CENTERS IN THE SCIENTIFIC INFORMATION INFRASTRUCTURE

E.A. Isaev[1,2,4,5], M.B. Amzarkov[2,3], V.D. Pugachev[1,2,5], V.A. Samodurov[1,2], R.R. Sukhov[2,3], N.A. Kobylka[2,4], Yu.A. Tarasova[2], E.Yu. Assur[5]

[1] Pushchino Radio Astronomy Observatory ASC LPI, Pushchino, Russia, *is@itaec.ru*
[2] National research university Higher school of economics, Moscow, Russia
[3] Uptime Technology INO, Moscow, Russia
[4] Stack Group, Moscow, Russia
[5] Itaec, Pushchino, Russia

ABSTRACT. There is a multiple increase of the volume of scientific data obtained in the course of research each year. Due to this there is a need for continuous improvement, such as data transmission channels and systems for handling and storage of scientific data. For example, data centers show current centers and storage of scientific data and advanced technology in this area, in particular the "cloud" technology. Particular attention is paid to the information infrastructure for data centers storing scientific information.

Key words: Data center.

Due to the multiple increase every year volumes of scientific data collected during the research, there is need for continuous improvement of channels for the transmission of such data as centers of scientific data.

The structure of a typical data center consists of:

1. Information infrastructure that includes server hardware and provides the core functionality of the data center - data processing and storage.
2. Telecommunications infrastructure for the interconnection of elements of the data center, as well as transfer of data between the data center and users.
3. Engineering infrastructure for the proper functioning of the main systems of the data center.

Classification of data centers:

a) in size;

b) the reliability;

c) for other purposes.

In more detail a typical example of a scientific-buffered data center data center space project "Radioastron" on PRAO ASC LPI (www.prao.ru). Data center is located in the building of an international test site project space radio telescope "Radioastron." For the placement of the data center has been allocated a special room where the server onto your mounted, uninterruptible power supply and cooling system. Data center PRAM has two storage servers with a capacity of 24 and 48 terabytes.

The next example of a modern data center is a parallel computing system (cluster) Pushchino Research Center (PSC), RAS, which was established in 2000 by the Institute of Mathematical Problems. The necessity of his appearance dictated by the demand solutions to many demanding computing tasks assigned research and educational groups PSC RAS.

Then move on to a modern network of commercial data centers Stack Data Network (SDN), which is Russia's first fault-tolerant network of data centers, in the design and development of which international best practice and experience of DC-outsourcing in Russia are reflected. Network uptime data centers SDN ensure geographical remoteness of its nodes and highly redundant core engineering systems (according to a N +1). One of the five data centers is located in the city of science SDN Pushchino. Pushchino and institutions have Sciences Centre's start to use these computing resources.

As an overseas data center is a typical example of the Harvard-MIT Data Center (HMDC, www.hmdc.harvard.edu), who is a member of the Institute IQSS. It was created in the early 1960s as a data center for Political and Social Sciences at Harvard University. Over the years into a HMDC information service and technology provider for social research and education for many departments, centers and research projects at the Faculty of Arts and Sciences and other schools at Harvard.

METHODS CONTROL RADIOASTRONOMY OBSERVATIONS AND PROCESSING OF COSMIC RADIO SOURCES

E.A. Isaev[1,2]

[1] Pushchino Radio Astronomy Observatory ASC LPI, Pushchino, Russia, *is@itaec.ru*
[2] National research university Higher school of economics, Moscow, Russia

ABSTRACT. In this paper the following methods represented: control of the radio astronomical observations using the estimation results, making decisions on the detection of cosmic sources, taking into account noise and interference, and recognizers classes of cosmic radio sources to the maximum of a posteriori probability (Bayesian approach). The problem researched is about storing and transferring large amounts of scientific information from cosmic radio sources to consumers.

Key words: information systems, computational biology, parallel processing system.

The method control of radio astronomical observations using the estimation results, which will significantly increase the efficiency of radio astronomical observations is considered in this work. There is a wide variety of assessment systems that require management procedures. On the other hand, there is not a smaller variety of control systems that require the estimation procedure. Schemes of these systems are provided.

In theory of detection and estimation of the parameters of radio signals some models are used. The model should, on the one hand, meet demand of its proximity to the real signal, and on the other hand allow you to carry out a theoretical analysis, which can be extended to more general cases. The method of decision making of detection of cosmic radio sources considering the noise and interference with the detection of the optimality criterion according to which you can choose the best one (likelihood ratio).

We use Bayesian approach for the method of recognition for classes of cosmic radio sources to the maximum of posteriori probabilities. The Bayesian approach is based on the theorem, which states that if the frequency function of each class is known, the required algorithm can be written in explicit analytic form. Moreover, this algorithm is optimal, ie, it has a minimal error rate.

Breakthrough in electronics, computing and information technology over the past 50 years have led to the fact that one of the dominant trends in modern science is the significant increase in the recorded and received data and the associated problems of storage and processing of this information. Synthesis of science and IT leads to the realization of the fact that a significant breakthrough in the knowledge of the world is possible only in case of possibility of processing of extra-large amounts of information and that the role of information and its processing in research is crucial. In particular, astronomers have faced with the fact that they need to handle the flow of information to several terabytes per day (more on the sites http://www.astrogrid.org/ and http://www.euro-vo.org/). Approximately everywhere, especially in research, there is a rapid replacement of the analog digital technologies. Examples of these trends in radio can be projects of unique and ambitious generation of radio telescopes: Atacama Large Millimeter Array (ALMA), Square Kilometer Array (SKA), Low Frequency Array (LOFAR) and others. This paper investigated on modern radiotelescopes task processing, storage and transmission of radio astronomical data.

THE CROSS-IDENTIFICATION, VISUALIZATION AND COMPARATIVE ANALYSIS OF ASTRONOMICAL CATALOGS IN A COMMON DATABASE RADC

M.A.Kitaeva [1,3], V.A.Samodurov [1,2,4], D.V.Dumsky [1], E.A.Isaev [1,2], V.D.Pugachev [1,2]
[1] Pushchino Radio Astronomy Observatory of Lebedev Physical Institute, Russian Academy of Sciences (Pushchino, Russia)
[2] National research university Higher school of economics (Moscow, Russia)
[3] marina@prao.ru, [4] sam@prao.ru

ABSTRACT. The Pushchino Observatory of ASC LPI have been developing in some last years database of some astronomical catalogs (Radio Astronomy Data Center – RADC, look on http://astro.prao.ru/db/ and http://observations.prao.ru/). In the database have the most commonly used by radio astronomers data: survey catalogs of radio sources at different radio frequencies (as well as in other spectral bands), catalogs of the major sky objects studied in astronomy etc.

Key words: radio survey, astronomy catalogues, database

The Pushchino Observatory of ASC LPI has database of some astronomical catalogs and observatory observations (Radio Astronomy Data Center – RADC, look on http://astro.prao.ru/db/ and http://observations.prao.ru/).

Since 2011 the database of astronomical catalogs actively equipped visualization of data and compare catalogs between them. These funds will provide the basis for statistical analysis and cross-sectional analysis of various astronomical catalogs.

For this task we have developed the Graphical data representing from several catalogs within the chosen area on the sky, the map data and the statistical analysis of the main parameters as for each catalog as a whole, also as statistics cross-identifications of the user's favorite catalogs. At the moment the database will is improved by advanced visualization of individual radio sources as a result of identification in the elected by user catalogs (flux distribution over the frequencies, the distribution of spectral indexes, etc.).

Work was supported by the program of the Presidium of RAS "The origin, evolution and structure of objects in the universe," and program of the Department of Physical Sciences "Active processes and stochastic structures in the universe."

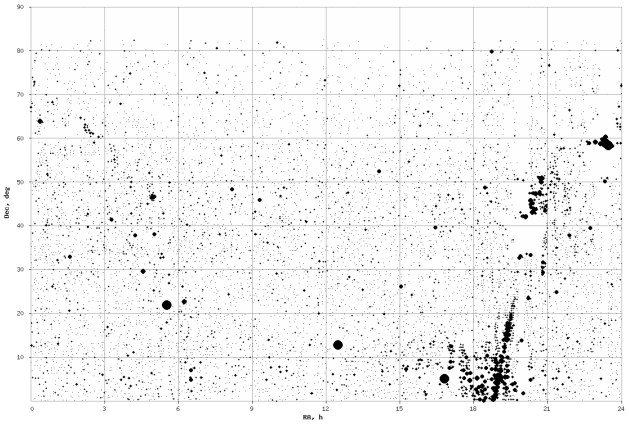

Figure 1: The example NSS102 radio catalog map. It is represented all sources of Pushchino catalog at 102 MHz with declination more than 0 degrees.

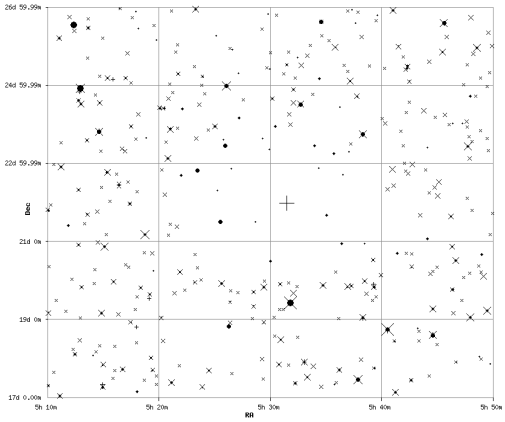

Figure 2: The example of a comparing of the data sky fields for three catalogues: 4C (178 MHz, by direct cross) 1400 MHz (circles) and GB6 (4850 MHz, oblique crosses). There are zone of avoidance near strong source that showed only in 4C catalog.

MODERN INFORMATION SYSTEMS FOR RESEARCH WORKS OF THE PUSHCHINO RESEARCH CENTER OF RAS

V.V. Kornilov[1,2,4], E.A. Isaev[1,3,4]

[1] Institute of Mathematical Problems of Biology RAS, Pushchino, Russia, *basil@psn.ru*
[2] Pushchino State Institute of Natural Science, Pushchino, Russia
[3] Pushchino Radio Astronomy Observatory ASC LPI, Pushchino, Russia, *is@itaec.ru*
[4] National research university Higher school of economics, Moscow, Russia

ABSTRACT. The current state of information systems of the Pushchino Research Center of the Russian Academy of Sciences allows us to successfully solve the problems of computational biology.

Key words: information systems, computational biology, parallel processing system.

The Pushchino Research Center (PRC) of the Russian Academy of Sciences (RAS) includes 9 institutes of RAS focusing on microbiology, molecular biology and biophysics and the Radioastronomical Station of the Astrocosmic Center of the Physics Institute. On the basis of the institutes of the PRC two universities: Pushchino State Institute of Natural Science and a branch of Moscow State University are working. PRC is a unique formation of global significance and has around about half of Russia's potential in the field of Physical and Chemical Biology.

At present the solution of problems in biology, especially in computational biology: bioinformatics, structural and computational genomics, molecular modeling, is needed for the use of powerful computing and communications resources. To successfully conduct the research on a global level the modern biologist needs a high-speed access to information contained in the world databases via Internet, high-speed processing of large volumes of data, using supercomputers with the goal of computer modelling of biological systems and so on.

In recent years, a great amount of work to meet these requirements has been done. Now all the institutes of PRC as well as educational foundations, data storage and data processing systems are combined into a single local area network built on fiber optical channels. It has high-speed access to Internet via optical communication channel with data rate 10 Gbit/s. It allows not only to find necessary information in the world wide web but to work with supercomputing centers such as Joint Supercomputer Center of RAS, supercomputer Lomonosov of Moscow State University, other Russian and foreign supercomputer centers.

The powerful parallel processing system (cluster) are working in PRC RAS on the basis of the Institute of Mathematical Problems of Biology to meet the acute need of PRC researchers for highly efficient computational resources so that they might solve numerous computational problems requiring mass computer memory and high speed of operation. At the present time the overall cluster performance is about 900 Gflops. In the further plans of improvement of the performance of the cluster is considered to increase the number of computing nodes and upgrade the internal cluster network.

Due to the organization of GRID-infrastructure developing within the framework of funded by EU project EGEE, enormous computational capacities and huge information volumes will be reachable for all scientific community.

In Pushchino State Institute of Natural Science successfully conducted training and graduate students with advanced multimedia teaching computer classes.

A number of other projects for creation and development of modern information systems are made and continued.

The direct optical channel from tracking station RT-22 in Pushchino to Moscow processing center has been created and put into operation to transfer large amounts of data at the final stage of the establishment of ground infrastructure for the international space project "Radioastron". A separate backup system for processing and storing data is organized in Pushchino Radio Astronomy Observatory to eliminate data loss during communication sessions with the Space Telescope.

IONOSPHERE DISTURBANCES OBSERVATIONS DURING THE PERIOD OF SOLAR ACTIVITY MAXIMUM

Kravetz R.O.[1], Galanin V.V.[2]

Institute of Radio Astronomy of National Academy of Science of Ukraine,
Odessa, Ukraine
[1]krro@ukr.net, [2]gvv@mail.ru

ABSTRACT. Strong ionosphere disturbances dates in the first half of 2012 year are defined on the data of ionosonds network. Sporadic E_s layer appearance and strong radio wave absorption phenomena, when the reflections from ionosphere are completely absence, are studied. We show, that frequency and duration of ionosphere disturbances are increased in summer months compare to winter ones.

Key words: ionosphere, ionogram

Ionosphere observations are provided for a long time and are an actual problem. It take place mostly because of ionosphere have a significant effect on radio communications in various frequency ranges. For the radio astronomy the ionosphere has also great importance, because it can significantly distort signals from cosmic radio sources, which is received by the earth based radio telescopes. The most serious distortions are appeared during the disturbances in ionosphere. So the problem of observation and registration of ionosphere disturbances are very important.

The base instrument for ionosphere observation is the ionosphere stations (ionosonds) network, which give all ionosphere parameters in real time. Results of ionosond measures are fixed on the ionograms, which represents the dependence of signals, reflected from ionosphere from the transmitted frequency

Most ionosondes in Europe are uniting in the common system named DIAS (European Digital Upper Atmosphere Server) [1, 2]. The data, provided by this system allow to estimate enough good ionosphere conditions, and particularly, to define presence of disturbances. In this work we use data mostly from Warsaw ionosond.

Ionosphere disturbances observations are in particular interest during the solar activity maximum, because in this period the number and the intensity of ionosphere disturbances are increased as a rule. In this work we study ionosphere disturbances, which occurred in the first half of 2012 year, i.e. in the period of solar activity maximum or the period that is closely precede to it.

The ionospheres disturbances are often connect with the varying of F2 layer critical frequency over it mean value. Such disturbances can be positive (when the critical frequency increase) or negative (when the critical frequency decrease). Ionosphere disturbances caused in most times by the solar flares and their consequences [3]. After the strong solar flare the X-ray stream is appear, then it reaches Earth and caused higher ionization of ionosphere (mostly of D layer). Such disturbances named sudden ionosphere disturbances. Something later the stream of particles, mainly protons, are reaches the Earth, and they also cause higher ionization and respectively ionosphere disturbances. But such disturbances are take place only on the high latitudes.

Other type of ionosphere disturbances is caused by magnetic storms [3], which lead to electron concentration changes and so to increase of radio waves absorption.

Along with the above mentioned types of ionosphere disturbances we may consider such phenomena as an E_s sporadic layer. This layer is not regular and it can appear in any time of the day and in any time of the year. Duration of it existence is not big and can be from some minutes to some hours. However, because of high electron concentration in this layer, it can significantly influence on the radio waves spreading. Particularly, when sounding ionosphere from the Earth, it can black out higher layers. On the other side, when the radio waves come from the space, as it take place during the radio astronomy observations, they may not reach the Earth. So, sporadic layer E_s appearance can significantly influence on the radio astronomy observations, and it study is very important.

The typical example of sporadic layer E_s appearance is showed on the figure 1, where some consequent ionorams are presented. Ionograms interval is 15 minutes. Sporadic layer E_s appeared as a horizontal strait trace and reflections from higher layers are absent because of black out effect. Within near half an hour, sporadic layer E_s is disappear and ionograms becomes to its original form.

From ionograms of the first half of year 2012 there was defined all dates of sporadic layer E_s appearance and it's approximately times of appearance and durations. This data is presented in table 1.

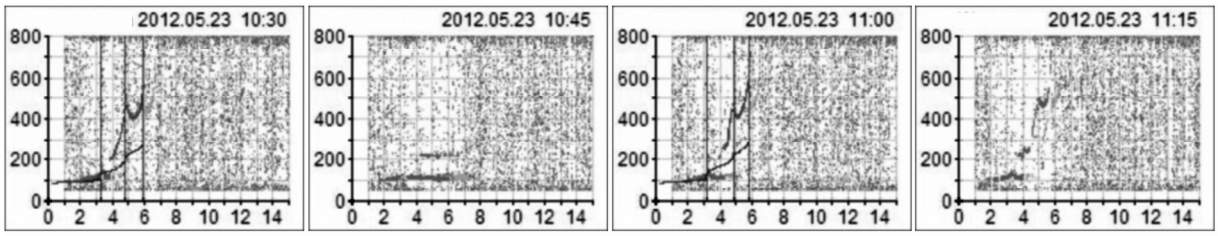

Figure 1: Ionograms 23.05.2012. Sporadic layer E_s appearance.

Table 1: Dates, time of appearance and durations of sporadic layer E_s in the first half of year 2012.

DATE	TIME	Duration	DATE	TIME	duration	DATE	TIME	duration
January 02	15:00	1	May 01	18:45	1	June 04	17:30	0.5
05	17:00	1	02	19:15	0.5	06	10:45	1
07	20:00	1	05	10:00	1.5	09	17:30	1
07	22:00	0.5	10	23:00	3	10	05:15	3
15	19:00	0.5	11	00:00	1	11	07:45	2
16	20:00	0.5	14	12:00	0.5	12	06:45	2
17	05:30	0.5	17	16:30	1	12	10:45	2
19	17:30	1.5	18	22:15	0.5	14	19:45	0.5
23	04:00	1	23	10:45	0.3	15	10:30	1
February 08	04:30	1	24	03:15	1.5	17	07:00	1
20	21:30	0.5	27	19:15	1	17	17:30	1
March 02	11:00	1	27	23:00	0.5	18	00:30	0.5
April 01	21:45	1	28	02:15	1	19	03:00	1
29	19:00	0.5	28	06:15	1	26	07:00	2
30	09:45	0.5	28	17:00	3	27	15:30	2.5
			28	17:00	3	28	17:00	1
			29	17:45	1	29	08:00	0.5
			29	23:15	1	29	14:30	3
			31	20:15	0.45	30	16:00	2

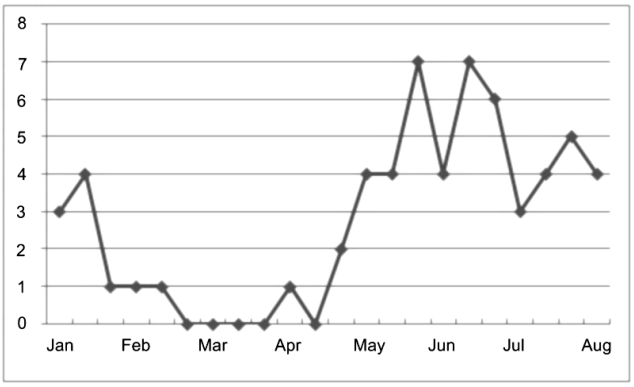

Figure 2: Sporadic layer E_s appearance frequency.

Also there was calculated approximately values of frequency of sporadic layer E_s appearance. Thees values were calculated as a ratio of number of days, when the sporadic layer E_s layer appears, to all days of observations in decade. This data is presented on figure 2. This plot shows that in summer months (beginning from May) the frequency of sporadic layer E_s appearance is significantly higher than in winter ones. Duration of sporadic layer E_s existence is also higher in summer month than in winter ones. The most notable days were July 2 and 17, when sporadic layer E_s was practically continuously exist for 10 and12 hours respectively.

When ionograms was analyzed, there was find some phenomena of strong radio wave absorption, when reflections from ionosphere are completely absent (so called black-outs). Example of such phenomena showed on figure 3. For the comparison, figure 4 show ionograms made in the same time of previous day, when the disturbance was absent. Such phenomena were observed several times during the given period.

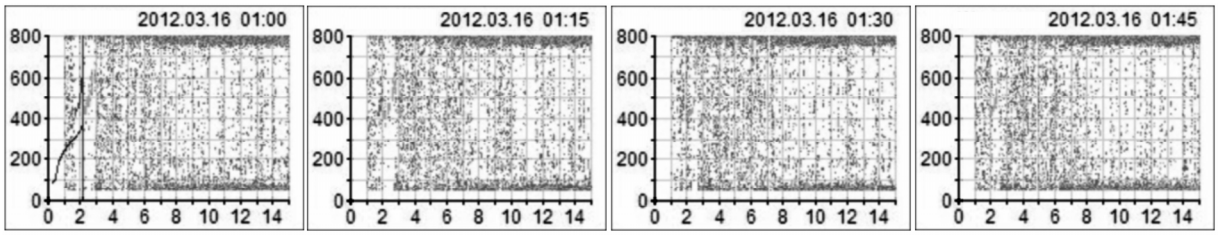

Figure 3. Ionograms 16.03.2012. Reflections from ionosphere are absent.

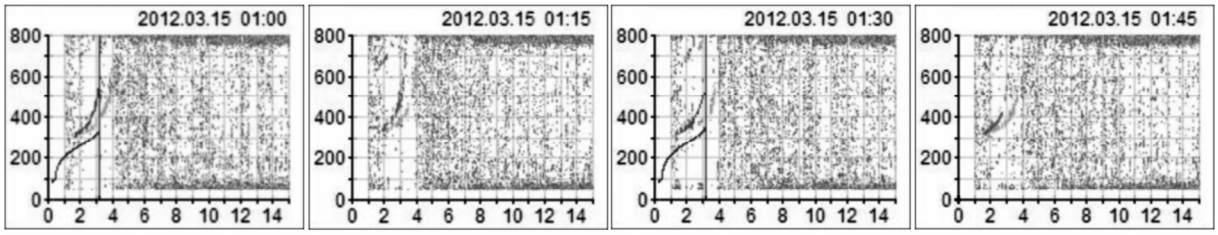

Fig.4. Ionograms 15.03.2012. Ordinary reflections from ionosphere.

The strongest effects of such type was observed on Mach 16, when reflections from ionosphere was absent for 2.5 hours, and on July 15, when reflections was absent for 2 hours. Similar phenomena were observed on January 24, April 24 and July 9, 11 and 19.

References

1. DIAS: European Digital Upper Atmosphere Server. *http://www.iono.noa.gr/dias*.
2. Belehaki A., Cander Lj. R., Zolesi B., Bremer J., Jurén C., Stanislawska I., Dialetis D., Hatzopoulos M.: 2005, *J. Atmos. Sol-Terr. Phys.*, **67(12)**, 1092.
3. Brjunelli B.E., Namgaladze A.A.: 1988, *Physics of Ionosphere*, M., Nauka.

GEMINGA: NEW OBSERVATIONS AT LOW RADIO FREQUENCIES

V.M .Malofeev [1], O.I. Malov, S.V. Logvinenko, D.A. Teplykh [2]
Pushchino Radio Astronomy Observatory, Lebedev Physical Institute,
142290, Pushchino, Moscow reg., RUSSIA
[1] *malofeev@prao.ru,* [2] *teplykh@prao.ru*

ABSTRACT. After nearly 10 years, we have succeeded to detect radio emission from Geminga more again. In this report we present new evidence for presence of radio emission from Geminga in the range 42-112 MHz. The observations were carried out on two sensitive transit radio telescopes We used three new digital receivers to detect the pulses and to obtain dynamic spectra.The examples of mean pulse profiles are presented. Exact value of the dispersion measure have been calculated using the simultaneous observations at three frequencies.

Keywords: pulsars, radio emission.

Introduction

Geminga was discovered in gamma-ray in 1975 (Fichtel et al., 1975). For a long time this source was remained unidentified until its detection as X-ray pulsar (Halpern & Holt, 1992) and slightly late as gamma-ray pulsar (Bertsch et al., 1992) with a period of 237 ms. All attempts to detect the radio source or pulsar have been unsuccessful till 1997, when three group from Pushchino Observatory (Astro Space Center, Lebedev Physical Institute, Russia) reported the detection of pulsed radio emission from Geminga at frequency 102.5 MHz (Malofeev & Malov 1997; Kuzmin & Losovsky 1997; Shitov & Pugachev 1998). In 1999 presence of radio emission were conformed at the same frequency 103 MHz (Vats et al., 1999). At now there is no evidence for detections of radio emission at more high frequency. But recently the weak continuum radio emission has been detected at the frequency 4.8 GHz (Pellizzoni et al., 2011).

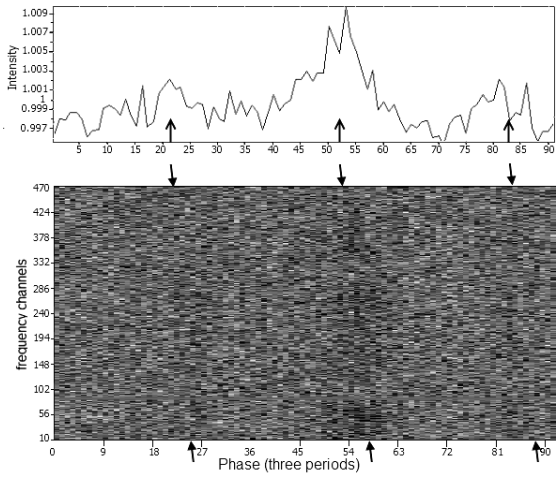

Figure 1: Example of a pulse profile (upper) and a dynamical spectrum (lower) of Geminga at 111 MHz, obtained by summing 36 selected groups (triple periods) on the 20.01.12. The horizontal axis is in samples of the triple period of the pulsar. The dispersion track is marked by arrows.

Observations and results

The observations were carried out on two sensitive transit radio telescopes in Pushchino in the range 42-112 MHz. First of them is Large Phase Array (LPA) antenna, with operating frequency 111.5±1.5 MHz and the effective area $3 \cdot 10^4$ m^2. Second one is DKR-1000 (East - West arm), which operates at 30-110 MHz and has the effective area ~ 7000 m^2. New series of observations was obtained using a unique set of digital, multi-channel receivers designed for pulsar observations, which came into use in 2006-09. The spectrum of the signal is calculated using an instrumental realization of a 1024-point FFT processor. The time resolution that can be obtained is 0.2048 ms. The width of the operational frequency band is 2.5 MHz, which is separated by the FFT into 512 spectral channels with widths of 4.88 kHz each. The reduction programs implement several techniques for removing interference, using several criteria for distinguishing false pulses from real signals (see, for detail, (Malofeev et al. 2012)).

We continued the observations of Geminga at low radio frequencies and hoped to detect strong signal, but did not reported most of unsuccessful observations or the seldom week pulses. Suddenly in the beginning of this year new observations in Pushchino showed the evidence for the detection of Geminga at three low frequencies during two months (January-February of 2012) in a few sets of observations. Here, we present the results for three days 19 — 21 of January integrated profiles of selected groups at all three frequencies (Fig. 1-3). To check the presence the weak pulsar signal and to raise the reliability we determine the observing window or the group as three apparent pulsar period with the sampling interval 7.5776 ms. One observation set contained 280 or 841 groups (triple periods) at frequencies 111 MHz and 42/62 MHz accordingly. The direct integration of all groups showed weak signal with signal-to-noise ratio (S/N) about 5 in some observations. But if we used the method of visible pulses selection (Malofeev et al. 2012) for reduction of data in these observations, the value of S/N ratio can reach more than 10 in these days (Fig.1,3).

In this case we summed all group, where have been the pulses with S/N > 2 at selected phase. The mean profile of 36 selected groups is presented at Fig.1 (upper). Here the integration was carried out at phase sample 52 ± 3, but possible see two other more week pulses at the phases near samples 21 and 83. All three pulses are separated by one pulse period (31.29 samples). Next method was the summing of selected groups with pulses, which show S/N > 2 in folding profile for the observing window as one pulsar period, as shown in Fig.2b. This selection showed the presence of three pulses in the observing window (Fig. 2-3). Both types of selected groups of integration

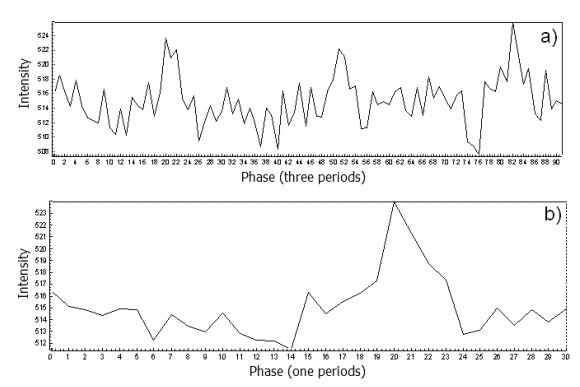

Figure 2: (a) Example of a pulse profile of Geminga at 62 MHz, obtained by summing 20 selected groups (triple periods) on the 20.01.12. (b) The mean profile for one period obtained by the folding of data. The horizontal axis is in samples of the triple period (a) and one period (b) of the pulsar.

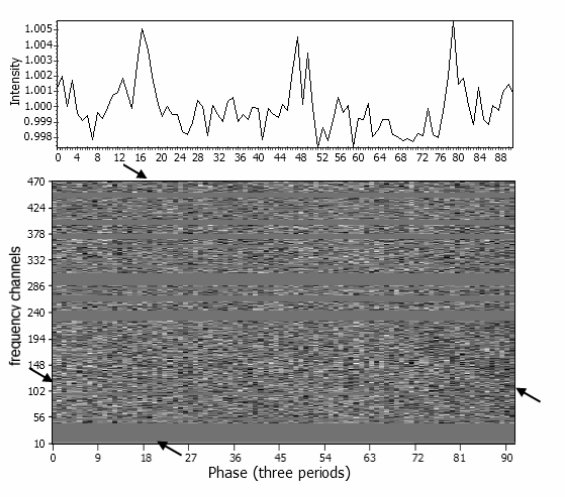

Figure 3: Example of a pulse profile (upper) and a dynamical spectrum (lower) of Geminga at 42 MHz, obtained by summing 23 selected groups (triple periods) on the 21.01.12. The dispersion tracks are marked by arrows.

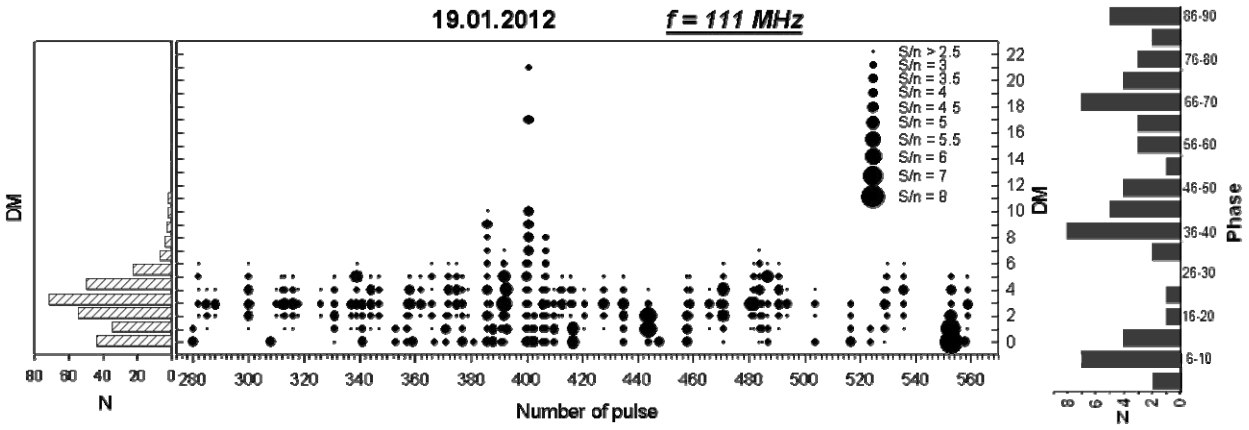

Figure 4: The central panel shows events with $S/N > 2.5$ at different DM versus number at pulse (time) (size of the circle indicates the value of the signal to noise ratio). The left panel shows the histogram of the number of events vs DM. The right panel shows histogram of the events with $S/N > 2.5$ versus of period phase for 19.01.2012 (triple period).

demonstrates the presence of periodical radio emission from Geminga at low frequencies. Next very important thing is the presence of the signal dispersion. We have been luck and first time new simultaneous observation at three frequencies on 20 of January give us possibility to measure more exactly the value of DM = 2.89 ± 0.02. The dispersion tracks are seen at dynamic spectra of Fig. 1,3 (bottom panels). Fig. 4 shows events with $S/N > 2.5$ in depend on number of pulse, DM and phase of period for 19.01.2012 at 111 MHz.

Conclusions

1. The presence of periodic radio emission has been confirmed at all three low frequencies.
2. We measured precise value of the dispersion measure (DM = 2.89 ± 0.02) using the simultaneous observations at three frequencies.
3. The long-term (a few years) intensity variation can be the cause of the absence of low frequency radio emission from Geminga during about 10 years.

Acknowledgments. This work was financially supported by the Russian Foundation for Basic Research (project code 12-02-00661) and Academy of Science (program nonstationary phenomenon in the objects of Universe 2012).

References

Bertsch D., et al.: 1992, *Nature*, **357**, 306.
Fichtel C.E., Hartman R.C., Kniffen D.A., et al.: 1975, *ApJ*, **198**, 163.
Halpern J., Holt S.: 1992, *Nature*, **357**, 222.
Kuzmin A., Losovsky B.: 1997, *Pis'ma AZh*, **23**, 323.
Malofeev V., Malov O.: 1997, *Nature*, **389**, 697.
Malofeev V., Teplykh D., Logvinenko S.: 2012, *Asron. Rep.*, **56**, 35.
Pellizzoni A., et al.: 2011, *MNRAS*, **416**, 45.
Shitov Y., Pugachev V.: 1998, *New Astronomy*, **3**, 101.
Vats H., Singal A., Deshpande M., et al.: 1999, *MNRAS*, **302**, 65.

OSCILLATIONS OF DECAMETER TYPE IV BURSTS OBSERVED ON APRIL 7, 2011

Melnik V.N.[1], Brazhenko A.I.[2], Konovalenko A.A.[1],
Panchenko M.[3], Frantsuzenko A.V.[2], Rucker H.O.[3]

[1] Institute of Radio Astronomy of NAS of Ukraine, Kharkov, Ukraine
[2] Poltava gravimetrical observatory of Institute of geophysics of NAS of Ukraine, Poltava, Ukraine
[3] Space Research Institute, Austrian Academy of Sciences, Graz, Austria

Introduction

The new branch of solar physics known as solar seismology (Nakariakov & Verwichte, 2005) reaches a huge progress last ten years. Since observations of oscillations and pulsations of different coronal structures (such as magnetic loops, prominences) become possible at the optical, x-ray and radio wavelength ranges with spacecrafts (TRACE, SOHO, SDO, etc). Analysis of obtained data gives an opportunity to estimate the plasma parameters of the source region using the theory of MHD oscillations. Periods of registered oscillations vary from several seconds to tens minutes. They are associated with fast magneto-acoustic, slow magneto-acoustic, Alfven and sound waves. There are some mentions (for example Mel'nik et al., 2008) about radio emission oscillations of the type IV bursts at the frequencies 10–30 MHz.

In this paper we consider oscillations of decameter radio emission of the type IV bursts registered on April 7, 2011 by the radio telescope URAN–2. Using Fourier and wavelet analyses we derive characteristic periods at different frequencies.

Observations and results

We registered decameter type IV bursts on the 7th of April, 2011 by radio telescope URAN–2 (Poltava, Ukraine) (Megn et al., 2003). In this day observations by URAN–2 were carried out from 06:12 to 14:02 UT.

There were two coronal mass ejections (CME) on April 7, 2011 according to SOHO. The first one propagated in southeast direction, and the second one moved in southwest direction. The first and the second type IV bursts were observed simultaneously with the first and the second CMEs.

In this paper we investigate oscillations with the largest periods. We used Fourier analysis and wavelet analysis. There are two main long-wave periods. The first one is near 75 minutes and associated with the first and the second bursts. The second long-wave period is near 40 minutes and related to the second event. We obtained that both periods decreased with time. Drift rate of the first period is 0.07. It changes from 88 minutes at the beginning of the first event to 77 minutes at the beginning of the second event and became stable till the end of the second burst. Drift rate of the second period is smaller. Its value is 0.06. This period changes from 47 minutes at the beginning to 38 minutes at the end.

Similar dependencies are obtained in the whole frequency band from 8 MHz to 32 MHz. These results are agreed by both Fourier and wavelet analyses.

Such long periods can be connected with oscillations of the CME core or very high magnetic arches. We show that more possible are oscillations of CME cores and they are associated with magneto-sound or Alfvenic waves. In the case of the first one the temperature of core plasma is $10^6 - 10^7 K$. If oscillations are connected with Alfvenic waves then for magnetic field surrounded the core we have 0.3–0.6 *G*. Both values and plasma density, and magnetic field are seen reasonable.

Conclusion

We discover radio emission oscillations of the decameter type IV bursts registered on April 7, 2011 by the radio telescope URAN–2. Fourier and wavelet analyses show the presence of oscillations with characteristic periods near 75 and 40 minutes. It seems that these are oscillations of CME cores.

References

Nakariakov V.M., Verwichte E.: 2005, *Living Rev. Sol. Phys*., **2**, 3-65.

Mel'nik V.N., Rucker H.O., Konovalenko A.A., Dorovskyy V.V., Abranin E.P., Brazhenko A.I., Thide B., Stanislavskyy A.A. Solar Type IV bursts at frequencies 10-30 MHz // *Pingzhi Wang Solar Physics Research Trends*. – NewYork: Nova Science Publishers, 2008. – P. 287-325.

Megn A.V., Sharykin N.K., Zaharenko V.V., Bulatsen V.G., Brazhenko A.I., Vaschishin R.V.: 2003, *Radio Physics and Radio Astronomy*, **8**, 345–356.

SOURCES WITH LOW-FREQUENCY STEEPNESS SPECTRUM CONCERNING THE UNIFIED MODEL

A.P. Miroshnichenko
Institute of Radio Astronomy of the NAS of Ukraine
Kharkov, Ukraine
mir@ri.kharkov.ua

ABSTRACT. Based on data of the data of the Grakovo catalogue of the extragalactic sources, detected at the decametre band with the UTR-2 radio telescope , it was established, that properties of radio sources with low-frequency steepness of spectrum are in accordance with the long evolution. At that, quasars and galaxies with low-frequency steep spectra often are the sources of the infrared and the X-ray radiation. In the last case we use the possibility of alternative determination of the magnetic field strength in the sources necessary for the estimate of the ratio of the magnetic field energy and the energy of the relativistic particles. Also we obtained the relations of sources luminosities at the radio, infrared, optical, X-ray bands that revealed evolution effects. The analysis of considered relations for quasars and galaxies with low-frequency steepness of radio spectrum testifies for the unified model of sources.

Key words: radio spectrum, quasar, galaxy, magnetic field strength

Introduction

Radio sources with low-frequency steepness spectrum (type C+) correspond to conception of the long evolution of this class of sources, when the critical frequency of the synchrotron emission can displace to values less than 10 MHz. Before [1] we received estimates of the main physical parameters of quasars and galaxies with steepness spectrum over the sample of objects at the decametre band (at that the value of low- frequency spectral index exceeds 1). The examined sample of objects with spectrum C+ is compiled at the base of the Grakovo catalogue of extragalactic sources detected with the UTR-2 telescope at the declination ranges $\delta = -13^0 ... + 20^0$ and $\delta = 30^0 ... 40^0$ with flux density more than 10 Jy at the frequency 25 MHz [1]. With given criteria 148 sources are selected, including 52 galaxies, 36 quasars and 60 optically non-identified objects. The optical and high-frequency data for sample sources have been get from the NED database (*http://nedwww.ipac.caltech.edu*). Note, that the redshift range of objects is enough vast and forms $z = 0.017....2.4$.

Calculations of the physical parameters of radio sources with spectrum C+ were carried out at the frame of ΛCDM -Universe model. These calculations showed, that galaxies and quasars of the sample have the great luminosity (by order of 10^{28} *W/Hz ster* at the frequency 25 MHz) and very extent radio structure with linear size by order of 1 Mpc and characteristic age by order of 100 million years [1].

Independent estimation of the magnetic field strength

Our further analysis of properties of considered sources with spectrum C+ reveals that 14 objects from 36 sample quasars are the infrared sources, and 15 objects from the sample are the X-ray sources. It is known that many extragalactic X-ray sources have the non-thermal X-ray spectrum. At the assumption that the X-ray emission of quasars and galaxies may be due to the inverse Compton scattering of radio photons of the microwave background by relativistic electrons, it is the independent estimation of the magnetic field strength of objects. To obtain the magnetic field strength B_{IC} (at the inverse Compton scattering) by the flux density of X-ray emission we transform the relation from [2]:

$$B_{IC} = ((5.05 \cdot 10^4)^{\alpha} \cdot 1.15 \cdot 10^{-16} \cdot (1+z)^{\alpha+3} \times \\ \times S_r \cdot \nu_r^{\alpha} \cdot S_X^{-1} \cdot \nu_X^{-\alpha})^{\frac{1}{\alpha+1}} (Gauss) \quad , \quad (1)$$

where all values are at the CGS system, α - is a spectral index of steep radio spectrum, z is a redshift of object, S_r is a flux density of radio emission at the frequency ν_r, S_X is a flux density of X-ray emission at the frequency ν_X. We accept $\nu_X = 2.42 \cdot 10^{17} Hz$ (at the energy of X-ray photons 1 keV), $\nu_r = 2.5 \cdot 10^7 Hz$ (decameter band). As a result of calculations from (1), we receive the estimates of the magnetic field strength for quasars (mean value) in the sample with spectrum C+: $\prec B_{IC} \succ = 1.03(\pm 0.45) \cdot 10^{-6} Gauss$, and for galaxies (mean value) in the sample with spectrum C+: $\prec B_{IC} = 0.67(\pm 0.25) \cdot 10^{-6} Gauss$. Let us compare these estimates with the values of the magnetic field strength *B,* derived by us for the same objects at the assumption about the equipartition of the magnetic field energy and the energy of relativistic particles in the sources [1]: $B = 6.15(\pm 0.30) \cdot 10^{-6} Gauss$ - for quasars in the sample with spectrum C+, $B = 8.14(\pm 0.58) \cdot 10^{-6} Gauss$ - for galaxies in the sample with spectrum C+. As one can see from the derived estimates, the value of magnetic field strength B_{IC} is, in average, by one order less than the value *B*, determined at the equipartition condition.

It is possible to estimate the energy of relativistic particles by the value B_{IC} and the value of radio

luminosity L [3] in sources. So, in our case, the energy of relativistic electrons in sources with spectrum C+ is:

$$W_e = \frac{10^{12}\cdot L}{B_{IC}^{3/2}}\cdot\frac{\nu_2^{(1/2)-\alpha}-\nu_1^{(1/2)-\alpha}}{\nu_2^{1-\alpha}-\nu_1^{1-\alpha}}\cdot\frac{2-2\alpha}{1-2\alpha}(erg) \quad , \quad (2)$$

where $\nu_1 = 10MHz$, $\nu_2 = 100MHz$. Note, that the energy of relativistic particles in sources, when take into account the relativistic protons, may be $W_p = 100\cdot W_e$. Then the mean values of the energy of relativistic particles with (2) are: $\prec W_p \succ = 3.32(\pm 1.72)\cdot 10^{63} erg$ (for quasars) and $\prec W_p \succ = 3.77(\pm 1.55)\cdot 10^{61} erg$ (for galaxies) in the examined sample. It is known that the magnetic field energy in sources is:

$$W_{IC} = \frac{B_{IC}^2}{8\pi}\cdot V(erg) \quad , \quad (3)$$

where V is the volume of a source. The mean values of the magnetic field energy from (3) are: $\prec W_{B_{IC}} \succ = 1.19(\pm 1.13)\cdot 10^{62} erg$ (for quasars) and $\prec W_{B_{IC}} \succ = 9.35(\pm 4.05)\cdot 10^{58} erg$ (for galaxies) in the examined sample.

It turned out, that the mean values of the ratio of the magnetic field energy and the energy of relativistic particles for sources with spectrum C+ are: $\prec W_{B_{IC}} / W_p \succ = 0.13(\pm 0.07)$ (for quasars) and $\prec W_{B_{IC}} / W_p \succ = 0.91(\pm 0.81)$ (for galaxies) in this sample. So, we conclude from these ratios about the prevalence of the energy of relativistic particles over the energy of the magnetic field in the examined sources. The great extent of radio structure (~1Mpc) of quasars and galaxies with steepness spectrum at the decameter band may evidence in favor of such situation.

Ratios of emission at the different bands

Also, we examine the estimates of ratios of flux densities of emission in the different bands: decameter (frequency 25 MHz), centimeter (frequency 5000 MHz), infrared (IR), optical (opt), X-ray band for quasars and galaxies of the sample (at the logarithmic scale). These are identical to the ratios of the corresponding monochromatic luminosities (Table 1).

One can see, the mean values of corresponding ratios for quasars and galaxies in Table1 have enough close quantities. In that case, the obtained characteristics of radio sources with spectrum C+ are in concordance with the unified model of sources [4, 5]. Also, it follows from the presented ratios (Table 1), that galaxies contain more dust (which is responsible for the infrared emission) than quasars.

Let us examine relations for derived characteristics of quasars and galaxies with spectrum C+. In particular, the relation of the ratio of monochromatic luminosities at the decameter and infrared bands versus the redshift for the sample objects is presented in Figure 1.

Table 1. Mean values of the ratios of monochromatic luminosities at the different bands for quasars and galaxies with spectrum C+

Mean value of the ratio	Quasars	Galaxies
$\prec \lg(\frac{S_{25}}{S_{5000}}) \succ$	1.69(±0.08)	1.74(±0.05)
$\prec \lg(\frac{S_{25}}{S_{IR}}) \succ$	4.30(±0.11)	3.67(± 0.19)
$\prec \lg(\frac{S_{25}}{S_{opt}}) \succ$	5.00(± 0.10)	5.15(± 0.12)
$\prec \lg(\frac{S_{25}}{S_{X}}) \succ$	7.78(± 0.17)	7.89(± 0.33)
$\prec \lg(\frac{S_{IR}}{S_{X}}) \succ$	3.54(± 0.20)	4.68(± 0.47)

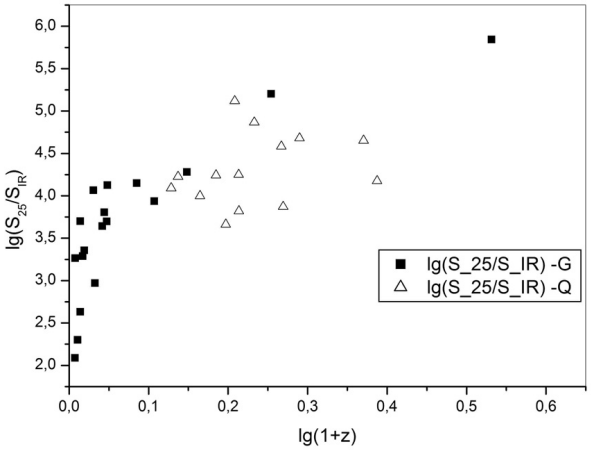

Figure 1: The ratio of monochromatic luminosities at the decameter and infrared bands versus the redshift

This relation evidences for the essential cosmological evolution of luminosities of sources with spectrum C+. The analogous picture is displayed in the relation of monochromatic luminosities of the sample objects at the decametre and optical bands versus the redshift (Figure 2).

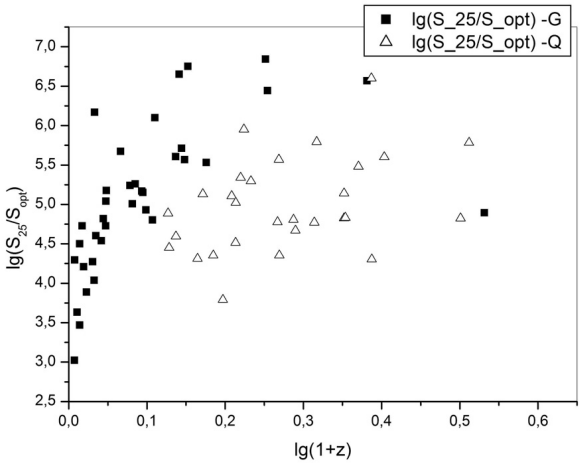

Figure 2: The ratio of monochromatic luminosities at the decameter and optical bands versus the redshift

The trend to increase of contribution of the decameter emission for more extent sources is noticeable in the relation of monochromatic luminosities versus the linear size of sources with spectrum C+ (Figure 3, Figure 4). The mutual relation of the monochromatic luminosities (Figure 5) for galaxies and quasars with spectrum C+ perhaps has maximum, indicating on the recurrence of the source's activity at the different bands.

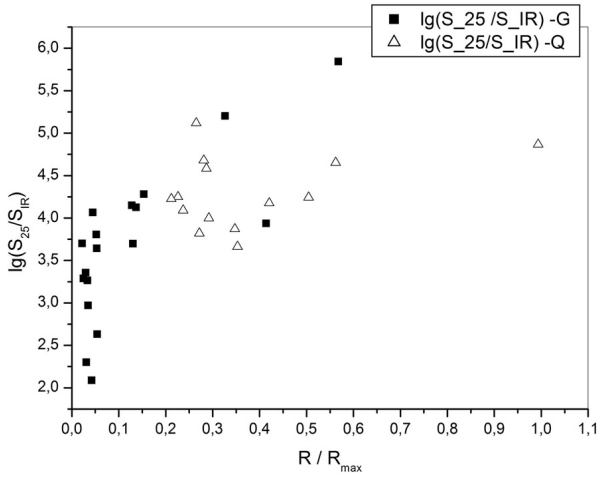

Figure 3: The ratio of monochromatic luminosities at the decameter and infrared bands versus the linear size

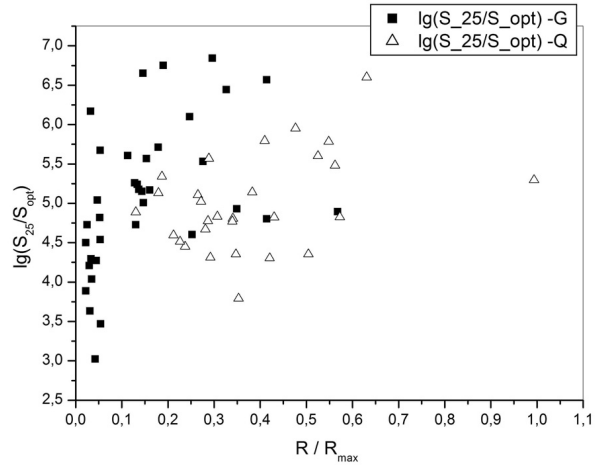

Figure 4: The ratio of monochromatic luminosities at the decameter and optical bands versus the linear size

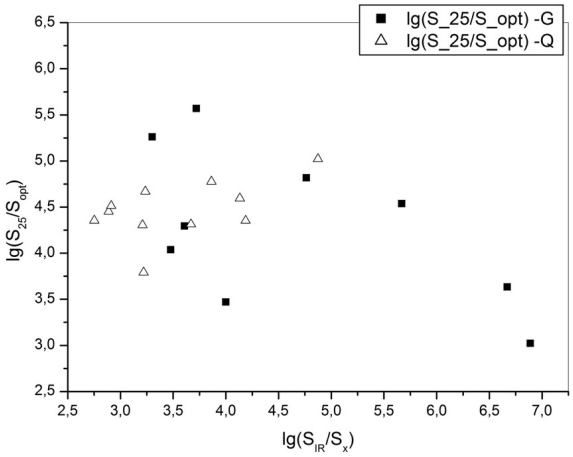

Figure 5: The mutual relation of monochromatic luminosities for the sample objects

Conclusion

The independent estimation of the magnetic field strength of the sources with spectrum C+ have been derived at the assumption about inverse Compton scattering for the X-ray emission of sources.

The contribution of the decameter emission increases for more extent sources with spectrum C+ and displays the evolution.

Similarity of the structure and the physical characteristics of galaxies and quasars with spectrum C+ testifies for the independence from the power of active nuclei and corresponds to the unified model of sources.

References

1. Miroshnichenko A.: 2012, *Radio Physics and Radio Astronomy*, **3**, 215.
2. Harris D., Grindley J.: 1979, *MNRAS*, **188**, 25.
3. Lang K.: 1974, *Astrophysical Formulae*, Berlin: Springer-Verlag.
4. Antonucci R.: 1993, *ARA&A*, **31**, 473.
5. Urry C., Padovani P.: 1995, *PASP*, **107**, 803.

VARIABILITY OF THE EXTRAGALACTIC RADIO SOURCES 3C120, CTA102, DA55 AND OJ287 ON CENTIMETER WAVES AND ITS CONNECTIONS WITH THE DATA OF VLBI OBSERVATIONS

M. Ryabov [1], A. Donskyh [2], A. Suharev [1], M. Aller [3]

[1] Odessa observatory "URAN-4" of the Radio-astronomical institute NAS Ukraine
[2] I.I.Mechnikov Odessa National University
[3] Radio observatory of Michigan University, Ann Arbor, USA

ABSTRACT. By data of the long-term monitoring (30-40 years) fluxes of extragalactic radio sources 3C120, CTA102, DA55 and OJ287 received on the RT-26, University of Michigan present results of data processing with use the wavelet analysis. Received analysis of trend and short-time components of the flux density changes in the studied frequencies 14.5, 8 and 4.8 GHz. For each time components on all frequencies found values of main periods and time of their existence, integrated power spectra for the phases activity for radio sources was built. From the results of VLBI observations in sources with long jets (3C120 and CTA102) detected quasi-periodic structures brighter components. Their appearance is linked to the dynamics of the interaction of shock waves in the jet emission from the cores. Quasi-periodic structures in the jet can be formed as a result of a return standing wave.

Introduction

Radio galaxy 3C120. Main characteristics: z ~ 0.033, the distance to the object ~142 Mpc. The observations were made at a frequency 14.5 GHz 33 years (1978–2011), 8 GHz 45 years (1966–2011) and 4.8 GHz 29 years (1980–2009). Diagram of the flux density at 3 frequencies for the common observation periods is presented in Fig. 1.

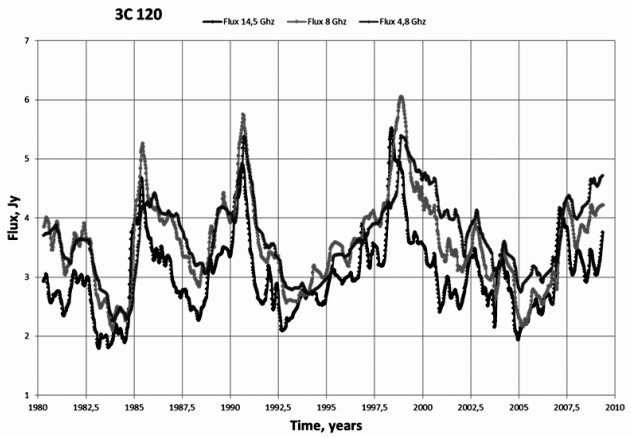

Figure 1: Graph of the fluxes at frequencies of 14.5, 8, 4.8 GHz, for the radio galaxy 3C120.

Quasar CTA102. Main characteristics: z ~ 1.037, the distance to the object ~6942 Mpc. For the source CTA102 data were obtained at frequencies of 4.8, 8 and 14.5 GHz for the 12-year period of observation (1999–2011).

Quasar DA55. Main characteristics: z ~ 0.859, the distance to the object ~5489 Mpc. For a source DA55 used data obtained at frequencies 4.8, 8 and 14.5 GHz for the 12-year period of observation (1999–2011).

Radio Source OJ287 refers to blazars, which are rapidly variability across the electromagnetic spectrum. Main characteristics: z ~ 0.306, the distance to the object ~1576 Mpc. We used the results of 30 years' observations (1979-2010) at frequencies 4.8, 8 and 14.5 GHz.

Observations

Investigation results monitored the 14.5, 8, 4.8 GHz fluxes of 3C 120, CTA 102, DA55, OJ 287 with the 26 m antenna of the University of Michigan Radio Astronomy Observatory. Details of the calibration and analysis techniques are described in Aller et al. (1985).

We used the average values of the fluxes of sources at regular intervals samples every 7 days.

With the use of a polynomial moving average (half-width of the interval 5 points), there was a decrease of noise and remove the casual bursts . Total flux densities of a radio source 3C120 are shown in Fig. 1. Allocation of short-component signals against the main period performed using Fourier filtering (O – C) (Gaydyshev, 2001). The change in the flux of sources at different frequencies has been observed mainly in time shift from the larger to the smaller frequency. The individual phases of activity sources can show the coincidence peaks at all frequencies.

FOURIER-analysis

In order to determine the periods Lomb-Scargle periodogram for data with an uneven readings on the time axis was built (Smolentsev, 2010). The spectral densities were calculated using the spectral Bartlet window. Examples of Fourier and wavelet spectra are shown in Fig. 2 and Fig. 3.

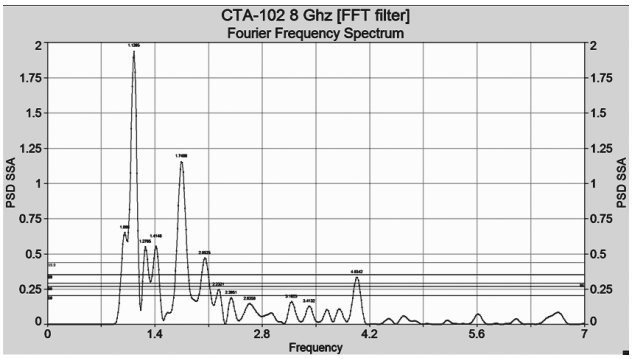

Figure 2: Periodogram for the source CTA102 at a frequency of 8 GHz.

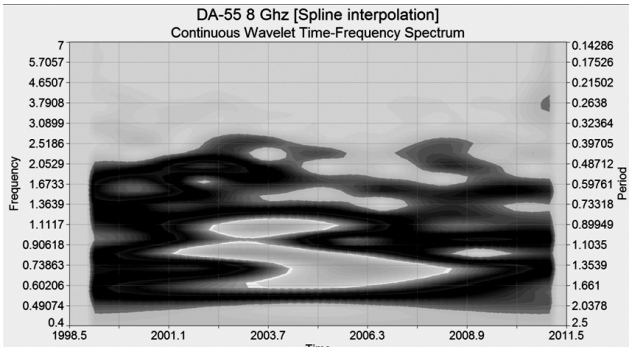

Figure 3: Continuous wavelet spectrum of the source of the «O – C» data for DA55, at 8 GHz.

WAVELET-analysis

Two-parameter analyzes function of one-dimensional wavelet transform is well localized in time and frequency. This distinguishes it from the ordinary Fourier analyzing function covers the entire time axis. Thus, it is possible to see the detailed structure of the process and the evolution of the harmonic components of the signal in time [4]. We used a continuous wavelet transform based on Morlet function. The example of the wavelet spectrum is shown in Fig. 4. On the wavelet spectra of the harmonic components of the signal are visible as bright spots, pulling in a strip along the time axis. The calculation of the integral wavelet spectra in the frequency range allows us to study the spectral variation of the signal power over time [3].

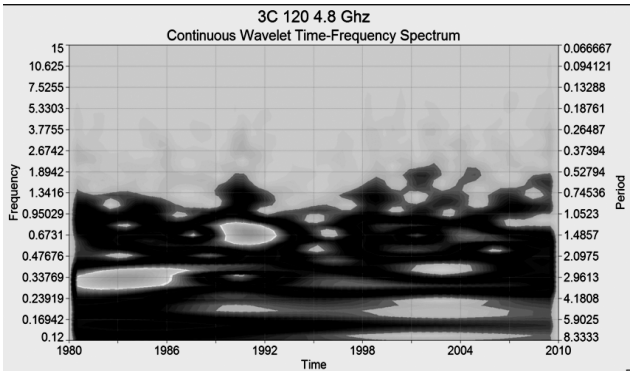

Figure 4: Continuous wavelet spectrum filtered series «O – C», for the source 3C120, at a frequency of 4.8 GHz.

Periods and phases of activity sources

3C120. The trend components.

The source 3C120 has a long-term 11 – 13-year-component at all frequencies. At 8 GHz found 24-year period. Phase of activity (bursts of spectral power) at the source 3C120 for the trend component observed at a frequency of 14.5 GHz – 1985, 1990 and 1998, at a frequency of 8 GHz – 1969 and 1974, at a frequency of 4.8 GHz -1990 and 1998 years.

Short periods (O – C). Periods about 2 and 5 years are also present at all frequencies. Similar values of periods 1.6 year (14.5 GHz), 1.3 year(8 GHz) and 1.6 year (4.8 GHz) may be a manifestation of the same process going on different frequencies. For the short-period component of this source activity phases were observed at a frequency of 14.5 GHz – 1990, 1992 and 1998, at a frequency of 8 GHz – 1990, 2004 and 2007, at a frequency of 4.8 GHz – 1990 year.

CTA102. The trend components.

The main period of the flux radio source is about 3 years. 2006 marked the largest phase of activity for the trend component at all frequencies.

Short periods (O – C). Source STA102 has components with periods 0.5 – 1 year. For the short-period component, activity phases were observed at a frequency of 14.5 GHz – in 2000, 2006 and 2009 years, at a frequency of 8 GHz – in 2009 and 2010 years , at a frequency of 4.8 GHz – in 2000.

DA55. The trend components.

There is long-period component of 6 – 8 years at all frequencies. For long-term component of the activity phases were of 14.5 GHz – in 2007 year, at a frequency of 8 GHz – 2004 and 2007 years, at a frequency of 4.8 GHz – in 2010.

Short periods (O – C). At all frequencies components 1 – 2 years and 3 years appear. Phase of activity for this components was observed at a frequency of 14.5 GHz – 1999, 2001, 2003 and 2010 years, at a frequency of 8 GHz – 2002, 2003 and 2005 years and at a frequency of 4.8 GHz – 2002 and 2010 years.

OJ287. The trend components.

At 8 and 14.5 GHz, the presence of 7 – to 8-year- long-period component. At frequencies of 4.8, 8 and 14.5 GHz 10 – 13-year component is shown. The peculiarity of this source in the presence of a trend at all frequencies. The period of this trend is likely to exceed 25 years.

Short periods (O – C). The source is the presence of 3-year component at frequencies 4.8, 8 and 22 GHz. At all frequencies the period of 1.6 to 1.1 years is changed. This change is the most evident in the frequency of 14.5 GHz. Phase of activity was at a frequency of 14.5 GHz – 1985 and 2010 years, at a frequency of 8 GHz – 1985 and 1989 years and at a frequency of 4.8 GHz – 1985 and 1989 years.

«Spectra periods»

For each year of observations graphics "spectra periods" were built to assess the contribution of individual periods in the activity of the radio source. In Fig. 5 shows an example of such a graph.

The use of a "spectrum of periods" allows comparisons with VLBI observations to determine the nature and dynamics of the processes in the jets.

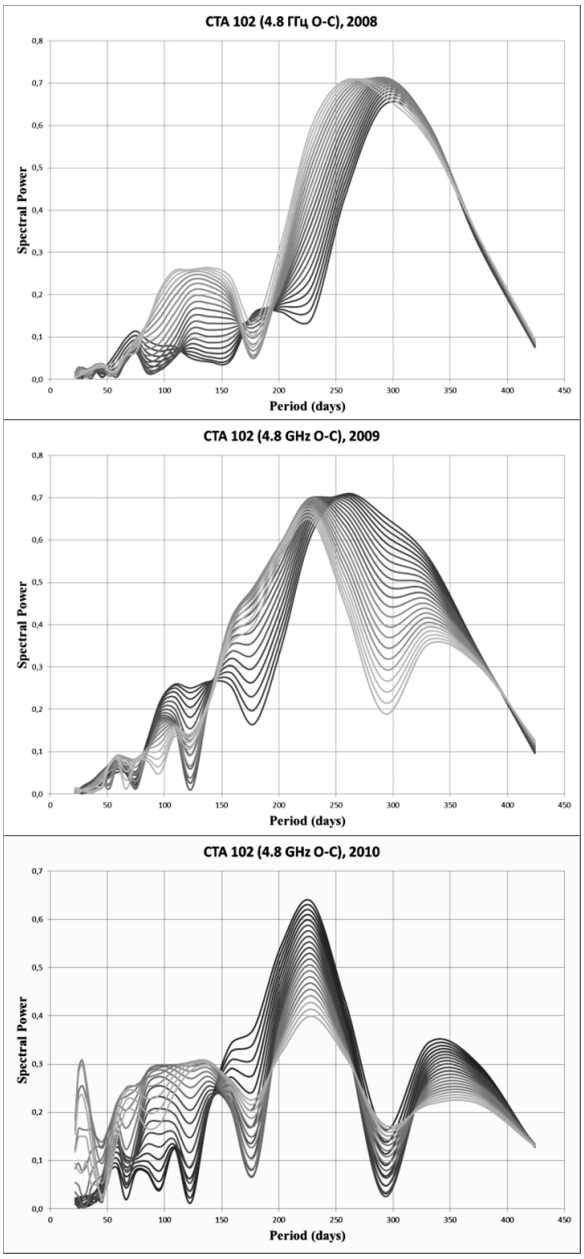

Figure 5: The graph shows the contributions of the individual periods in the activity of the radio source CTA 102 at a frequency of 4.8 GHz (O-C) for 2008–2010 years.

On the existence of quasi-stationary structures in the jets

In comparing the data on the availability of bright VLBI component in the jet being celebrated moving with time component and quasi-stationary structures bright knots occurring on the same distances from the cores. Such phenomena occur in sources with long jets 3C120 and CTA 102 (Fig. 6). Appearance of these nodes in the jets of brightness can be explained by a model of a standing backward wave.

Conclusions

Data processing based on wavelet analysis indicates the presence of a variable fluxes radio sources CTA102, 3C120, DA55 and OJ287 long-period and short components.

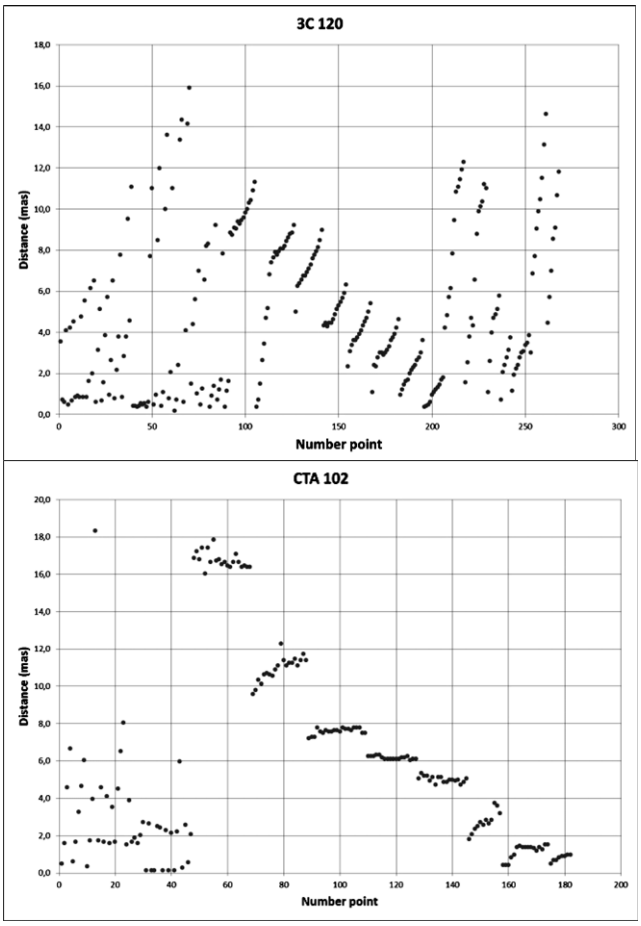

Figure 6: Quasi- stationary space structure of bright knots in the jet of 3C120 and CTA102.

Investigations the time of their existence, the main phases of activity and form the "spectra of periods." "The trend" component of the activity of radio fluxes formed by the long-term oscillations with a period in the range of 8 – 13 years or more. At the coincidence of the maxima of the trend component with maximum short-change flux with periods ranging from fractions to 3-year phase of the observed increased activity system «core- disk-jet». For each year of sources observations in all studied frequencies defined "spectra periods" determined by the contribution of the core and the jet activity. VLBI data show that the sources of 3C120 and STA102 with the activity of the cores are periodically increased flow from the jet. For sources DA55 and OJ287 core activity almost always prevails over the jet activity. In the VLBI data registration bright knots occur on the same distances from the core. This quasi-stationary structures found in jets from sources 3C120 and CTA 102.

References

Aller H.D., Aller M.F., Latimer G.E., Hodge P.E.: 1985, *ApJS*, **59**, 51.

Gaydyshev I.: 2001, Analysis and data processing (the special directory), St.Petersburg Publishing house.

Smolentsev N.: 2010, Veyvlet-analiz in MATLAB, DMK-Press.

RADIO VARIABILITY OF THE QUASAR 3C 273 ON THE CENTIMETRIC WAVES -WAVELET-ANALYSIS

Ryabov M. I. [1], SukharevA.L. [1], Sych R.A. [2]

[1] Odessa observatory "URAN-4" of the Radio-astronomical institute NAS Ukraine.
[2] Institute of solar and terrestrial physics, Siberian office Russian Academy of Sciences.
Aller M. F. Radio observatory of Michigan university, Ann Arbor, USA.

ABSTRACT. 3C 273– has been intensively investigated for many years, since opening of quasars in 1963. Since 1965 on radio telescope RT-26 of Michigan University on frequencies 14.5, 8 and 4.8 GHz long monitoring of this radio source have been carried out. Flux variability of a radio emission on studied frequencies consists a trend on which fast flux changes with characteristic time from 1 to 5 years are imposed. Fourier's methods and the wavelet-analysis that allowed investigating in details changes harmonious component of signals over time are applied. On a trend component the main period makes 8 years. With Fourier filtration have been received «O – C» data, for allocation high-frequency component in studied signals. By the results of calculations of wavelet-spectrums the periods of 3.5 and 2.3 years are revealed. On the basis of calculation of integrated wavelet-spectrums in a frequency range on «O – C» this «spectrum of the periods» characterizing main phases of activity of a source are defined. On the basis of the program written on IDL, supplementing the wavelet-analysis, delay change between fluxes on separate studied frequencies for each of periodic components has been defined eventually. The average delay for the 8 years periodic component in the range of frequencies of 4.8-8 GHz is about 1 year. In the range of frequencies 8 – to 14.5 GHz the average size of a delay was about 0.5 years. The average delay for all intervals of frequencies for the 3 years periodic components has appeared equal 0.3 years.

Introduction

3C273 – is the brightest quasar. It was opened in 1959. Main characteristics: red shift of Z ~ 0.16, visible magnitude V ~ 13, distance to object ~ 735 Mpc, mass of the central object of m ~ 886 million M_{SUN}, the linear extent of jet makes ~ 62 Kpc, the visible size – 23 ". Luminosity of the object changes in all a wave band from radio waves to range scale within about several days or ten days. Observation on VLBI has revealed own movements of some component in jet of 3C273 [1].

Data processing

On the basis of the carried-out daily observations average values in 7 days with a non-uniform grid of counting are defined. According to the histogram of distribution of time intervals between counting the interpolation interval in 0.02 years (7,3 days) has been chosen. With using a polynomial moving average (half width an interval of 5 points) reduction of noise has been reached and random emissions have been removed [2]. By means of trigonometrical interpolation data have been provided to an even step on time. The initial schedule with the combined frequencies is presented on fig. 1. The allocation of short periodic components of signals, which were imperceptible against the main period, has been carried out by Fourier filtration «O – C» [3].

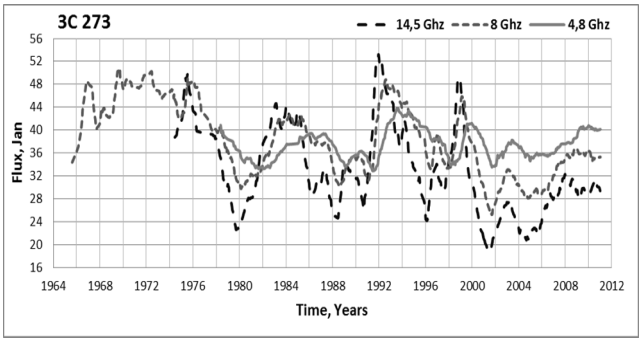

Figure 1: Monitoring of flux density quasar 3C 273 on 14.5, 8, 4.8 GHz.

FOURIER-analysis

For determination of values of the periods calculated Lomb-Scargle periodogram for data with non-uniformly located counting on time [4]. Frequencies with big spectral density, i.e. the frequency areas consisting of many close frequencies which make the greatest contribution to periodic behavior of all rows, were calculated with use of a Bartlett spectral window. Examples of Fourier and wavelet spectra are given on fig. 2 – 3. On all frequencies the most powerful period is close to 8 years. For «O – C» data the most appreciable periods with the values close by 2 and 3 years are found.

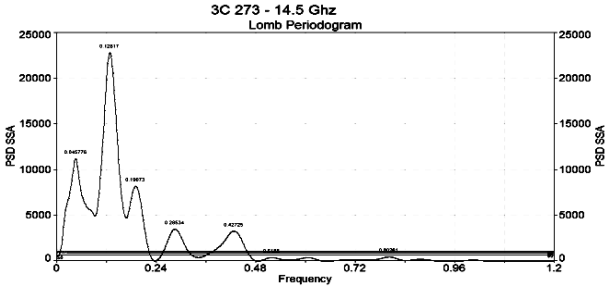

Figure 2: Periodogram for frequency of 14.5 GHz.

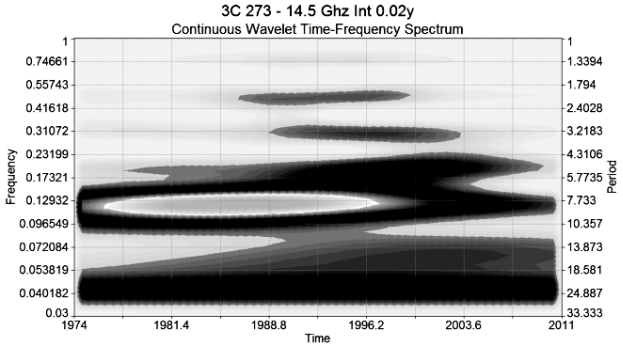

Figure 3: A continuous wavelet-spectrum of the initial smoothed data, frequency of 14.5 GHz.

WAVELET-analysis

Two-parametrical analyzing function of one-dimensional wavelet-transformation is well localized both in time and on frequency. That is distinguished from Fourier's usually applied transformation which analyzing function covers all time base. Thus it is possible to see detailed structure of process and evolution of a harmonious signal component in time [5]. Continuous wavelet-transformation on the basis of function Morlet was used. The example of a wavelet-spectrum is given on fig. 4. On wavelet-spectra harmonious components of a signal are visible in the form of the bright spots which are extending in strips along an axis of time.

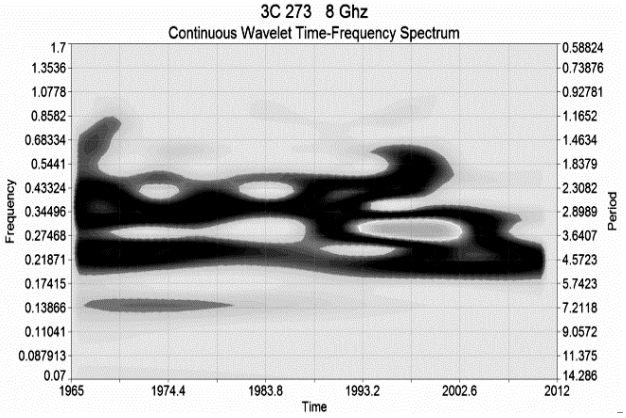

Figure 4: A continuous wavelet-spectrum for the filtered data «O – C», frequency of 8 GHz.

The analysis of ranges has shown existence in studied signals 8 years periods, and also the 3and 2 years periods, shorter periods with values are allocated about a year uncertainly and specification demand. Short time 2-3 years harmonicas are shown not on all length of a signal, and on its separate sites. Calculation of integrated wavelet-spectra in a frequency range for the filtered data has allowed studying change of spectral capacity of signals eventually. Activity phases (splashes in spectral power) were noted on frequency of 14.5 GHz – 1991.15, 1998.71 years; on frequency of 8 GHz – 1967.34, 1976.51, 1991.37, 1998.90; on frequency of 4.8 GHz – 1980.44, 1991.07, 1999.40. For each maximum on a global spectrum were constructed graphs of « spectrum of the periods», allowing to estimate a contribution of the separate periods to phases of activity of a radio source. On fig. 5 it is set an example such plot.

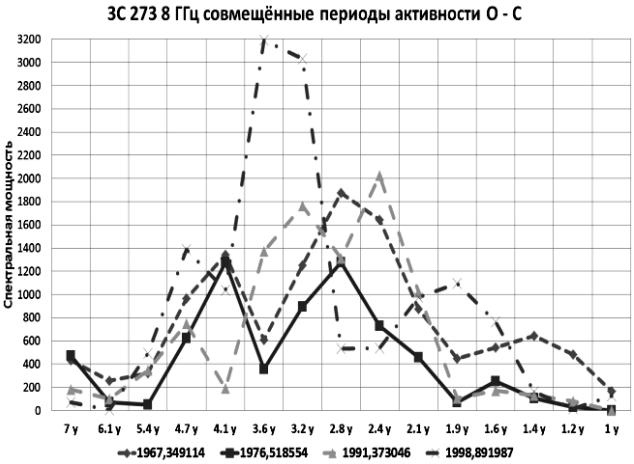

Fig. 5. On graphics contribution to of the separate periods to phases of activity of a radio source on frequency of 8 GHz are shown. For example, in a phase of activity of 1998.9 the most powerful period was of 3.6 years.

Use of «specter of the periods» allows to carry out comparison to data of VLBI observations and to define nature of dynamics of processes in jets. On the basis of the revealed regularities, it is possible to extend them to the entire period of the observation when sessions of VLBI of measurements were not.

Time delay between frequencies

For definition of delays between signals on different frequencies, calculation of direct and return wavelet-transformation was used [6]. This procedure is necessary for allocation of narrow-band signals of the found harmonicas and their comparison. Value of the strip wavelet-filter was fixed close ~ 3 and 8 years. The width of a window of the periods made 2 years. The capacity of fluctuations is non-uniformly distributed throughout the period of observation, there is their strengthening and the subsequent attenuation. For the period of 8 years this interval is in a range of 1979-2002, for the 3 years period

– in a range of 1986-2002. Then the time differences were found maximum and minimum of flux density for different spectral components. Values of positive half-cycles are designated by a dagger, negative are designated by a circle. On fig. 6 and 7 schedules of delays between frequencies for two allocated harmonicas are shown.

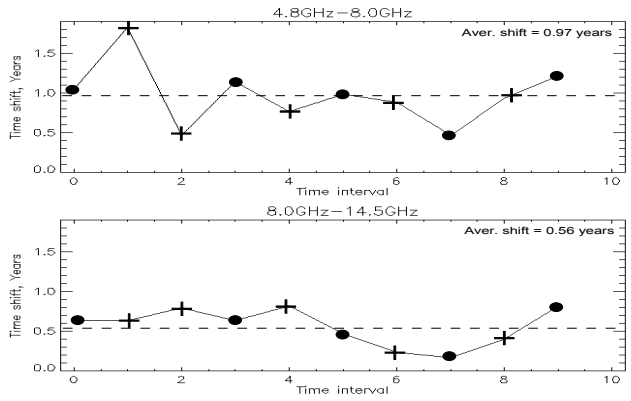

Figure 6: Delays between frequencies for a 8 years' period

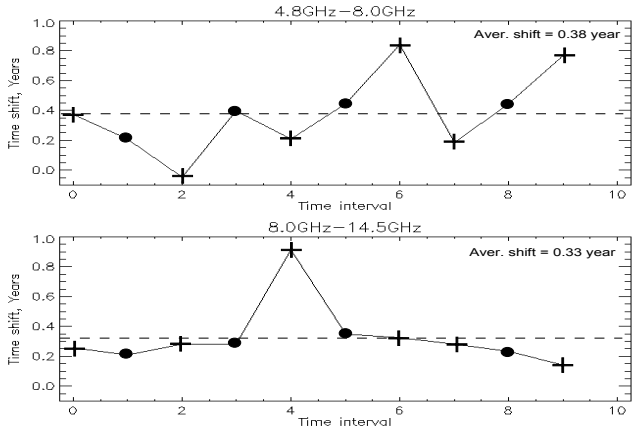

Figure 7: Delays between frequencies for a 3 years period

Conclusions

In this work, with using of a method of the wavelet-analysis existence of the 8 years' period on all studied frequencies that will be is consistent with results of other researches is defined. Fourier filtration method has allocated fast-variable components of signals with the periods of 3.5 and 2.3 years. Duration of the 3 years' period on frequency 14.5 GHz – 14.7 years, 8 GHz – 12.5 years, 4.8 GHz – 16.3 years. At a 8 years duration of manifestation on frequency 14.5 GHz – 14.3 years, 8 GHz – 15 years, 4.8 GHz – 13 years. On frequencies of 14.5 GHz and 8 GHz, probably, the period close to 5 years exist. Construct integrated wavelet-spectra in a frequency range for data «O – C». Activity phases of a source on frequency of 14.5 GHz are constructed – were shown in 1991.15, 1998.71 years. On frequency of 8 GHz in 1967.34, 1976.51, 1991.37, 1998.90 years. On frequency of 4.8 GHz – 1980.44, 1991.07, 1999.40 years. For each maximum on a global spectrum the schedules which allow to estimate a contribution of the separate periods to phases of activity of a radio source are constructed. The received results of delays between various frequencies of radio emission in a source 3C273 for the various periods allow to carry out further the detailed analysis of their physical reasons. For "trend" components with the period ~ time shift on frequencies in the range of 8 – 14.5 GHz twice are less than 8 years, than on lower frequencies (an interval of 4.8-8 GHz). Delays of high-frequency fluctuations do not show about 3 years change with frequency of generation. The average delay for the 8 year components in a range of 4.8-8 GHz is equal to 1 year, in a range 8 – 14.5 GHz a delay is about 0.5 years. An average delay for the 3 years components in all range of frequencies about 0.3 years. Long time changes of a radio flux 3C273 can be connected with quasiperiodic changes of rate of an accretion on a core [6]. 2 and the 3-year periods can be described by model of a shock wave in jet [7]. Variability models on the basis of a magnetic dynamo also well describe emergence of the short periods [8].

References

1. UchiyamaYa., Urry C.M., Cheung C.C., Jester S., Van Duyne J.: *Astrophys. J.*, **648** (2), 910.
2. Gaydyshev I. *Analysis and data processing* (the special directory), St. Petersburg Publishing house, 2001.
3. Davidov A.V. *Digital processing of signals: Thematic lectures*, Yekaterinburg: UGGU, IGIG, geoinformatics chair, 2007.
4. Vityazev V.V. *Analysis of non-uniform temporary ranks*, Publishing house of the St. Petersburg university, 2001.
5. Smolentsev N. *Veyvlet-analiz in MATLAB*, DMK-Press, 2010.
6. *Active kernels and star cosmogony* / Ed. Martynov. Publishing house of the Moscow university, 1987.
7. Marsher A.P.: 2006, in *confer. works: Astronomy 2006: traditions, present and future*, St.Petersburg State University.
8. Meyer F., Meyer-Hofmeister E. *The effect of disk magnetic fields on the truncation of geometrically thin disks in AGN.*

DATA PROCESSING CENTER FOR RADIOSTRON PROJECT

Shatskaya M.V.[1], Guirin I.A.[1], Isaev E.A.[2,3], Kostenko V.I.[1], Likhachev S.F.[1], Pimakov A.S.[1], Seliverstov S.I.[1], Fedorov N.A.[1]

[1] Astro Space Center LPI, Moscow, Russia, mshatsk@asc.rssi.ru
[2] Pushchino Radio Astronomy Observatory ASC LPI, Pushchino, Russia, is@itaec.ru
[3] National research university Higher school of economics, Moscow, Russia,

ABSTRACT. Radioastron is the international project led by the Astro Space Center of Lebedev Phisical Institute. Moscow, Russian Federation. 10 m Space Radio Telescope is the main payload of Spektr-R spacecraft. It's designed by Lavochkin Association of Roscosmos Russia State Agency. The project goal is to create together with a ground based radio telescopes the huge Ground to Space interferometer with a baseline up to 350 km, to obtain images, positions and movements of various objects in the Universe with extremely high angular resolution (about 10e–6 arcsec). After successful launch on 18 July, 2012 the Radioastron missions starts systematic investigations of the Universe at broad radio frequencies range.

DATA PROCESSING CENTER is a fail safe complex centralized system of interconnected software and hardware components, and organizational procedures, which is designed for reliable data storage and processing, delivery of services and applications, and this system possessed a high degree of virtualization of its resources. The main tasks performed by SDPC: effective realization of data acquisition and storage in a specialized data repository for a preset time with given reliability; delivery of applied services to users; and data processing on high performance computer complex.

The complex includes: control unit, computer cluster, data repository with a capacity of 200 TB, backup system on magnetic tapes (200 TB), 24 TB redundant storage system in the Pushchino Radio Astronomy Observatory, Astro Space Center of Lebedev Physical Institute in Pushchino, Web and FTP servers, networks of management and data transmission.

Let us consider each component of the computer complex in more detail.

The cluster (the main component of the complex) is a group of computers connected with high speed communication channels. From the standpoint of users it is an integrated hardware resource. The computer cluster presented in this paper includes one control and ten computing servers assembled in a common rack. Processing power of created computer cluster according to Linpack was found to be equal to 1000 Gflop/s.

The storage system consists of primary storage systems on 200 TB HDD plus 200 TB backup system. The first step for ensuring high availability is to protect the most important part of the system, namely, the data. Storage reliability is achieved by using RAID6 similar to RAID5, but having a higher degree of reliability: 2 disk capacity is allocated for check sums, double sums are calculated using different algorithms. This method suggests the use of disk arrays available to users as a single logical disk. The disk array has additional capacity providing for the ability of restoring the data in case of sudden failures.

In the case of failure of any component of the computer complex or its disconnection, a 24_TB data storage system organized in Pushchino can make backup in order to prevent data losses.

For prompt data exchange with backup data storage unit an independent direct communications channel with 1 GB/s speed was created between the Pushchino Radio Astronomy Observatory of Lebedev Physical Institute and Moscow Astro Space Center.

The information into the Processing Center comes via the Internet. From places, where there are no high speed communication channels, delivery of data on hard disks is possible.

The structure and functions of ASC Data Processing Center are fully adequate to the data processing requirements of the Radioastron Mission and has been successfully confirmed during Fringe Search and Early Science Program in flight operations.

References

Esepkina N.A., Korol'kov D.V., Pariiskii Yu.N., Radioteleskopy i radiometry (Radio Telescopes and Radiometers), Moscow: Nauka, 1973.

Thompson A.R., Moran J.M., Svenson G.W., Interferometry and Synthesis in Radio Astronomy, New York: John Wiley & Sons, 1990. Translated under the title Interferometriya i sintez v radioastronomii, Moscow: Fizmatlit, 2003.

Morimoto R., Noel M., Droubi O., Mistri R., Amaris C., Microsoft Windows Server 2008 Unleashed. Translated by OOO I.D. Williams, Moscow, 2009.